1917-C

Petrology, Diagenesis, and Sedimentology of Oil Reservoirs in Upper Cretaceous Shannon Sandstone Beds, Powder River Basin, Wyoming

U.S. GEOLOGICAL SURVEY BULLETIN 1917–C

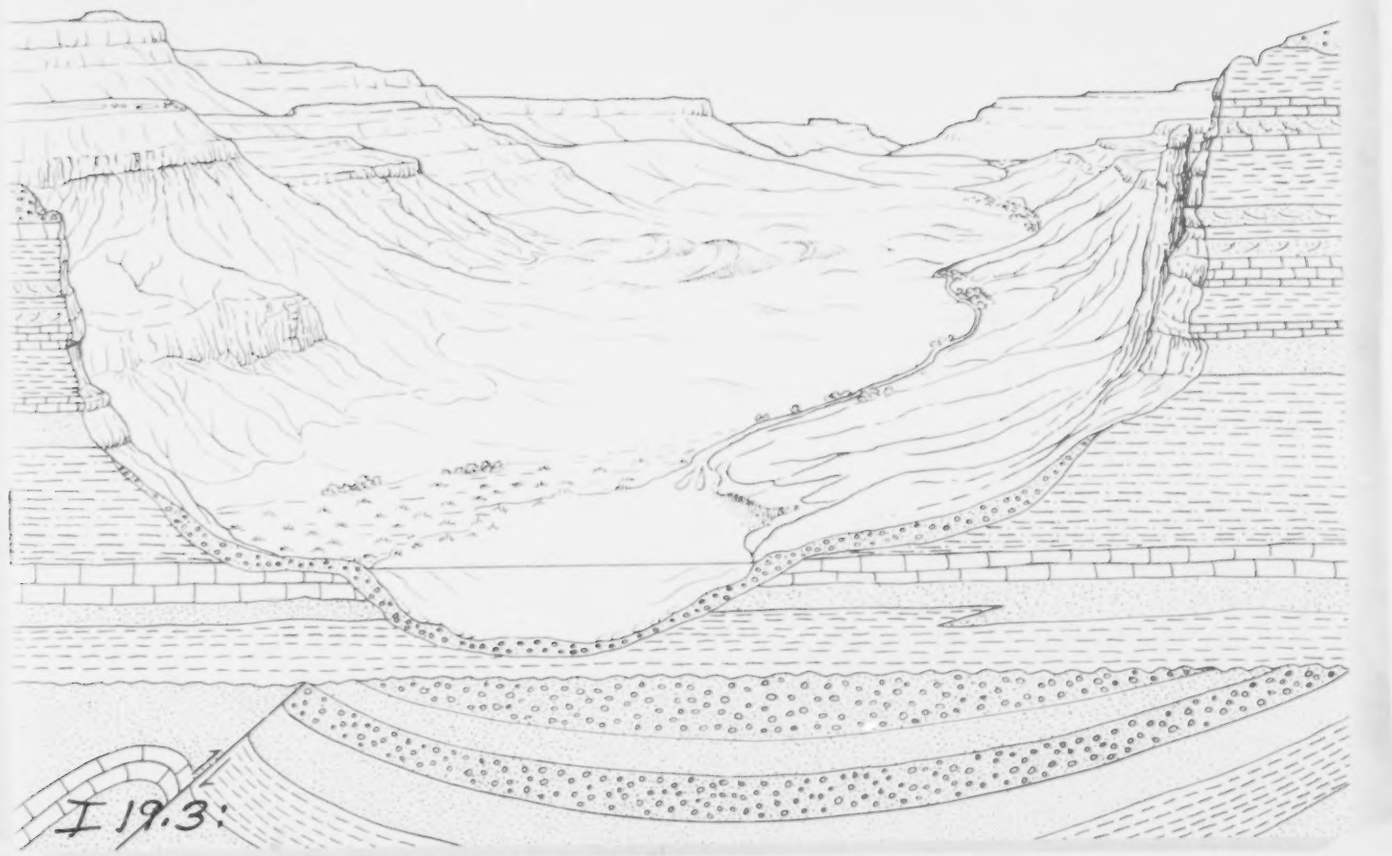

I 19.3:

best copy available

AVAILABILITY OF BOOKS AND MAPS OF THE U.S. GEOLOGICAL SURVEY

Instructions on ordering publications of the U.S. Geological Survey, along with prices of the last offerings, are given in the current-year issues of the monthly catalog "New Publications of the U.S. Geological Survey." Prices of available U.S. Geological Survey publications released prior to the current year are listed in the most recent annual "Price and Availability List." Publications that are listed in various U.S. Geological Survey catalogs (**see back inside cover**) but not listed in the most recent annual "Price and Availability List" are no longer available.

Prices of reports released to the open files are given in the listing "U.S. Geological Survey Open-File Reports," updated monthly, which is for sale in microfiche from the U.S. Geological Survey, Books and Open-File Reports Section, Federal Center, Box 25425, Denver, CO 80225. Reports released through the NTIS may be obtained by writing to the National Technical Information Service, U.S. Department of Commerce, Springfield, VA 22161; please include NTIS report number with inquiry.

Order U.S. Geological Survey publications **by mail** or **over the counter** from the offices given below.

BY MAIL

Books

Professional Papers, Bulletins, Water-Supply Papers, Techniques of Water-Resources Investigations, Circulars, publications of general interest (such as leaflets, pamphlets, booklets), single copies of Earthquakes & Volcanoes, Preliminary Determination of Epicenters, and some miscellaneous reports, including some of the foregoing series that have gone out of print at the Superintendent of Documents, are obtainable by mail from

U.S. Geological Survey, Books and Open-File Reports
Federal Center, Box 25425
Denver, CO 80225

Subscriptions to periodicals (Earthquakes & Volcanoes and Preliminary Determination of Epicenters) can be obtained ONLY from the

Superintendent of Documents
Government Printing Office
Washington, D.C. 20402

(Check or money order must be payable to Superintendent of Documents.)

Maps

For maps, address mail orders to

U.S. Geological Survey, Map Distribution
Federal Center, Box 25286
Denver, CO 80225

Residents of Alaska may order maps from

Alaska Distribution Section, U.S. Geological Survey,
New Federal Building - Box 12
101 Twelfth Ave., Fairbanks, AK 99701

OVER THE COUNTER

Books

Books of the U.S. Geological Survey are available over the counter at the following Geological Survey Public Inquiries Offices, all of which are authorized agents of the Superintendent of Documents:

- **WASHINGTON, D.C.**--Main Interior Bldg., 2600 corridor, 18th and C Sts., NW.
- **DENVER, Colorado**--Federal Bldg., Rm. 169, 1961 Stout St.
- **LOS ANGELES, California**--Federal Bldg., Rm. 7638, 300 N. Los Angeles St.
- **MENLO PARK, California**--Bldg. 3 (Stop 533), Rm. 3128, 345 Middlefield Rd.
- **RESTON, Virginia**--503 National Center, Rm. 1C402, 12201 Sunrise Valley Dr.
- **SALT LAKE CITY, Utah**--Federal Bldg., Rm. 8105, 125 South State St.
- **SAN FRANCISCO, California**--Customhouse, Rm. 504, 555 Battery St.
- **SPOKANE, Washington**--U.S. Courthouse, Rm. 678, West 920 Riverside Ave.
- **ANCHORAGE, Alaska**--Rm. 101, 4230 University Dr.
- **ANCHORAGE, Alaska**--Federal Bldg, Rm. E-146, 701 C St.

Maps

Maps may be purchased over the counter at the U.S. Geological Survey offices where books are sold (all addresses in above list) and at the following Geological Survey offices:

- **ROLLA, Missouri**--1400 Independence Rd.
- **DENVER, Colorado**--Map Distribution, Bldg. 810, Federal Center
- **FAIRBANKS, Alaska**--New Federal Bldg., 101 Twelfth Ave.

Chapter C

Petrology, Diagenesis, and Sedimentology of Oil Reservoirs in Upper Cretaceous Shannon Sandstone Beds, Powder River Basin, Wyoming

By PAULA L. HANSLEY and C. G. WHITNEY

A multidisciplinary approach to research studies of sedimentary rocks and their constituents and the evolution of sedimentary basins—both ancient and modern

U.S. GEOLOGICAL SURVEY BULLETIN 1917

EVOLUTION OF SEDIMENTARY BASINS—POWDER RIVER BASIN

DEPARTMENT OF THE INTERIOR
MANUEL LUJAN, JR., Secretary

U.S. GEOLOGICAL SURVEY
Dallas L. Peck, Director

Any use of trade, product, or firm names in this publication is for descriptive purposes only and does not imply endorsement by the U.S. Government.

UNITED STATES GOVERNMENT PRINTING OFFICE: 1990

For sale by the
Books and Open-File Reports Section
U.S. Geological Survey
Federal Center
Box 25425
Denver, CO 80225

Library of Congress Cataloging-in-Publication Data

Hansley, Paula L.
Petrology, diagenesis, and sedimentology of oil reservoirs in Upper Cretaceous Shannon Sandstone Beds, Powder River Basin, Wyoming / by Paula L. Hansley and C.G. Whitney.
p. cm. — (Evolution of sedimentary basins—Powder River Basin) (U.S. Geological Survey bulletin ; 1917–C)
"A multidisciplinary approach to research studies of sedimentary rocks and their constituents and the evolution of sedimentary basins—both ancient and modern."
Supt. of Docs. no.: I 19.3:1917C
1. Petroleum—Geology—Wyoming—Steele Shale. 2. Geology, Stratigraphic—Cretaceous. 3. Steele Shale (Wyo.) I. Whitney, Carroll Gene, 1949– . II. Title. III. Series. IV. Series: U.S. Geological Survey bulletin ; 1917–C.
QE75.B9 no. 1917–C
[TN870.5]
557.3 s—dc20
[553.2'8'09787]

90–3812
CIP

CONTENTS

Abstract C1
Introduction C1
Research design C3
Depositional environment C5
Sedimentology C6
Petrology C7
    Framework mineralogy C8
    Diagenetic alterations C9
        Siderite C10
        Pyrite C10
        Quartz C10
        Chlorite C10
        Calcite C11
        Glauconite-smectite C11
        Albite C14
        Minor authigenic phases C14
        Secondary porosity C14
        Oil C17
Isotopy C17
    Procedure C17
    Calcite C17
    Dolomite C19
    Siderite C20
Discussion C20
    Provenance C20
        Origin of glauconite C20
        Origin of dolomite C21
    Petrology of outcrop and core sandstones C23
    Diagenesis and paragenesis C24
    Depositional environment C27
        Mid-shelf model C27
        Alternative model C28
Conclusions C28
References cited C29
Appendix. Core descriptions of the Shannon Sandstone Beds of the Steele Member of the Cody Shale, Powder River Basin, Wyoming C32

FIGURES

1. Map showing locations of outcrops and drillholes from which samples of the Shannon Sandstone Beds of the Steele Member of the Cody Shale and the Groat Sandstone Bed of the Gammon Ferruginous Member of the Pierre Shale were collected in the Powder River Basin C2
2. Photograph showing outcrop of Shannon Sandstone Beds at the Salt Creek anticline C3

3. Chart showing stratigraphy of Upper Cretaceous rocks in the subsurface of the western part of the Powder River Basin **C3**
4. Map showing inferred paleogeography at the time of deposition of the Shannon Sandstone Beds **C5**
5–10. Photographs of core of the Shannon Sandstone Beds showing:
5. Facies 1a **C7**
6. Facies 2 **C7**
7. Facies 3 **C8**
8. Facies 4 **C8**
9. Bedded siderite in facies 4 **C9**
10. Coal partings at top of facies 2 **C10**
11. Diagram showing composition of sandstones from the Shannon and Groat Sandstone Beds **C11**
12. Plot of plagioclase versus potassium feldspar abundance, Shannon and Groat Sandstone Beds **C14**
13–15. Photomicrographs of:
13. Detrital glauconite grains and quartz **C15**
14. Dolomite grain and overgrowth **C15**
15. Detrital polycrystalline dolomite clast and quartz **C16**
16. Cathodoluminescence micrograph of detrital dolomite grains and overgrowths **C16**
17. Scanning electron micrograph of detrital dolomite grain and clay rim **C17**
18. Photograph of core of the Shannon Sandstone Beds showing detrital siderite clasts in facies 1a **C17**
19–20. Scanning electron X-ray fluorescence micrographs showing:
19. Siderite and calcite **C18**
20. Siderite overgrowth on dolomite **C18**
21–26. Scanning electron micrographs of:
21. Framboidal pyrite and quartz overgrowths **C19**
22. Authigenic pyrite and chlorite **C19**
23. Iron oxide pseudomorph after pyrite **C19**
24. Quartz overgrowth coated with oil **C19**
25. Etch pits in quartz overgrowth **C20**
26. Intergrowth of authigenic quartz and chlorite **C20**
27. Photomicrograph of authigenic chlorite rim under quartz overgrowth **C21**
28. Color photomicrograph and cathodoluminescence micrograph showing diagenesis of potassium feldspar **C22**
29. Scanning electron micrograph of highly diagenetically evolved glauconite **C23**
30. X-ray diffraction profiles of glauconite from deep and shallow sandstones of Shannon Sandstone Beds **C23**
31. Photomicrograph of chessboard albite **C23**
32. Scanning electron X-ray fluorescence micrographs of ferroan dolomite overgrowth on detrital dolomite grain **C23**
33. Scanning electron micrograph of skeletal plagioclase grain **C24**
34. Photomicrograph of oil between detrital quartz grain and quartz overgrowth **C25**
35. Diagram showing paragenesis of diagenetic alterations in the Shannon Sandstone Beds **C26**

TABLES

1. Outcrops and cores of the Shannon Sandstone Beds of the Steele Member of the Cody Shale and of the Groat Sandstone Bed of the Gammon Ferruginous Member of the Pierre Shale, Wyoming and Montana **C4**
2. Correlation of depositional facies in Shannon Sandstone Beds as described herein with facies as defined by Tillman and Martinsen (1984) **C6**
3. Point counts of selected thin sections of the Shannon Sandstone Beds and Groat Sandstone Bed, Powder River Basin **C12**
4. Identification criteria for detrital dolomite **C17**
5. Stable isotope values ($\delta^{13}C$ and $\delta^{18}O$) for calcite, dolomite, and siderite in Shannon Sandstone Beds **C25**

Petrology, Diagenesis, and Sedimentology of Oil Reservoirs in Upper Cretaceous Shannon Sandstone Beds, Powder River Basin, Wyoming

By Paula L. Hansley *and* C.G. Whitney

Abstract

The Shannon Sandstone Beds, which are contained within the Steele Member of the Upper Cretaceous Cody Shale, comprise linear, marine shelf sandstone ridges that contain productive oil reservoirs in the west-central Powder River Basin. Sandstones of the Shannon are mature litharenites dominated by chert fragments, glauconite pellets, and detrital dolomite grains and clasts. Detrital dolomite is a significant (as much as 15 percent) component of fine-grained sandstones. Diagenetic alterations in near-surface (< 100 m) sandstones are markedly different than alterations in deeply buried (> 2,500m) sandstones. Shallow sandstones contain unaltered framework grains that have floating and point contacts surrounded by calcite cement. In contrast, deeply buried sandstones are characterized by chlorite grain coatings, quartz and albite overgrowths, and extensive framework grain alteration—notably, detrital potassium feldspar grains partly to completely replaced by calcite. Interstratified glauconite-smectite, the major authigenic clay mineral in the Shannon, becomes less expandable with burial depth. Secondary porosity is locally abundant in shallow reservoirs, but secondary pores are commonly filled with authigenic minerals in deeper reservoir sandstones. Secondary porosity developed late in diagenesis and was followed by the late (?) Tertiary migration of oil into Shannon reservoirs.

The Shannon has been interpreted to be a mid-shelf marine sandstone that was deposited in at least 100 m of water. However, many characteristics of Shannon sand ridges are not satisfactorily explained by a mid-shelf model: abrupt changes of facies, abundant siderite and detrital dolomite, coal fragments and partings, juxtaposition of siderite and glauconite in crossbedded sandstones, and sideritic shale intervals barren of foraminifera. A possible alternative interpretation is that Shannon sand ridges were originally part of a linear shoreline sequence that was submerged during a transgression and then reshaped by longshore currents and marine organisms on the middle shelf.

Manuscript approved for publication February 19, 1990.

INTRODUCTION

Upper Cretaceous Shannon Sandstone Beds of the Steele Member of the Cody Shale form linear sandstone ridges that trend north-south in the west-central part of the Powder River Basin (fig. 1). The age of the Shannon as determined by potsssium-argon (K-Ar) dating of associated Upper Cretaceous bentonite beds is early Campanian, about 81 Ma (J.D. Obradovich, U.S. Geological Survey, Denver, oral commun., 1989). The Shannon crops out around the Salt Creek anticline in the southwestern part of the basin, where it consists of two stacked sand ridges (fig. 2), and at a few localities in Johnson County (Hose, 1955; Mapel, 1959; Gill and Burkholder, 1979) north of the Salt Creek area. In the subsurface, Shannon sand bodies are encased in shale (fig. 3), which provides a seal for stratigraphic traps from which oil is produced in many oil fields including Heldt Draw, Hartzog Draw, and Teapot Dome. Shannon reservoirs are less than 2 m to more than 20 m thick (Tillman and Martinsen, 1987).

The major goals of this study were to characterize the mineralogy and diagenesis of the Shannon in the Powder River Basin so that provenance, effects of organic acids on mineral diagenesis, and a paragenetic sequence of diagenetic alterations, including the relative timing of oil migration into Shannon reservoirs, could be determined. In addition, knowledge of the petrology and sedimentology of sand ridges such as the Shannon should lead to a better understanding of the genesis of sand ridges. Comparisons and contrasts between diagenetic

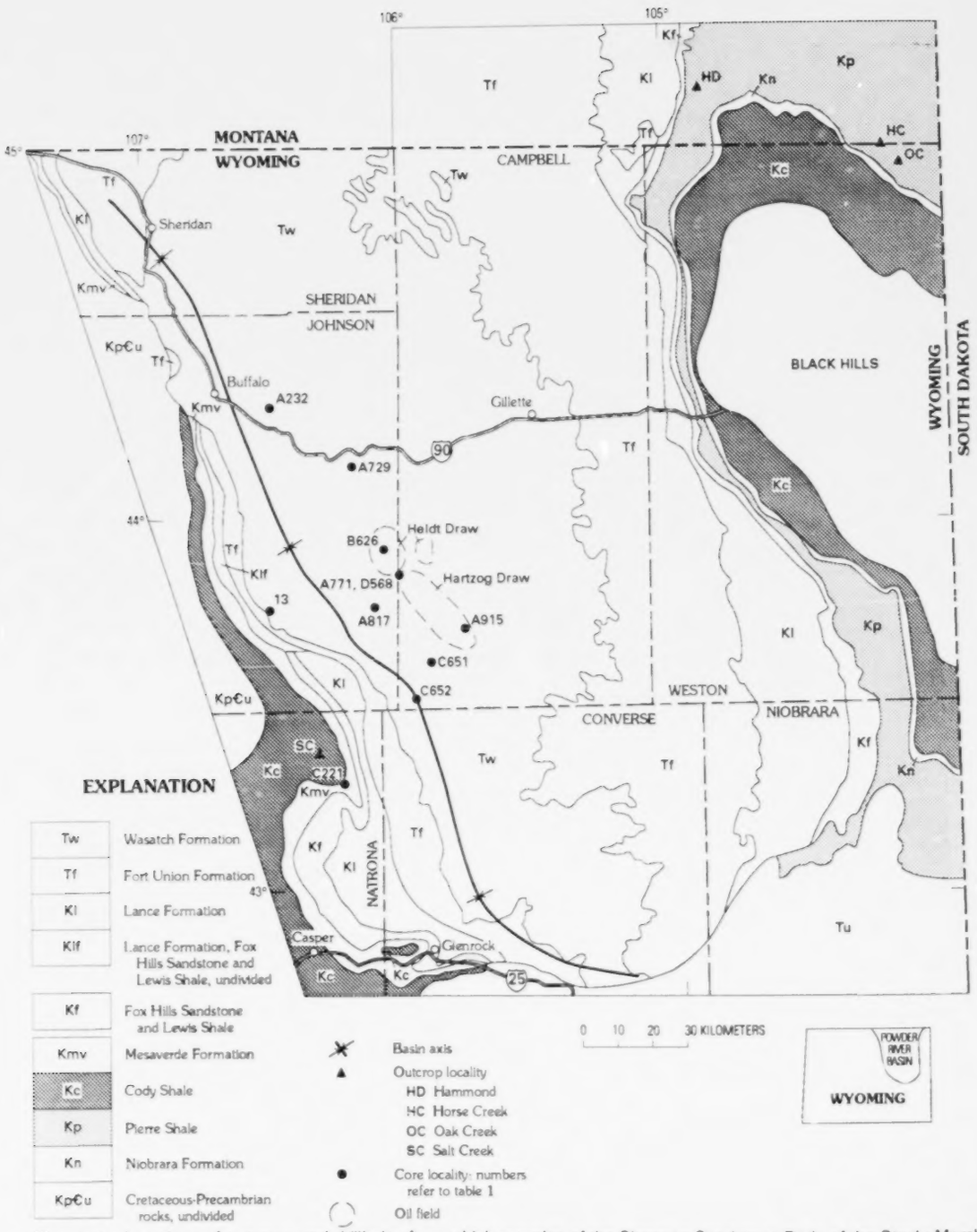

Figure 1. Locations of outcrops and drillholes from which samples of the Shannon Sandstone Beds of the Steele Member of the Cody Shale and the Groat Sandstone Bed of the Gammon Ferruginous Member of the Pierre Shale were collected in the Powder River Basin. Geology modified from Keefer (1974); geology of Black Hills not represented because of complexity and irrelevance to report.

Figure 2. Outcrop of Shannon Sandstone Beds showing facies 1, 2 and 3 at the Salt Creek anticline. Looking west.

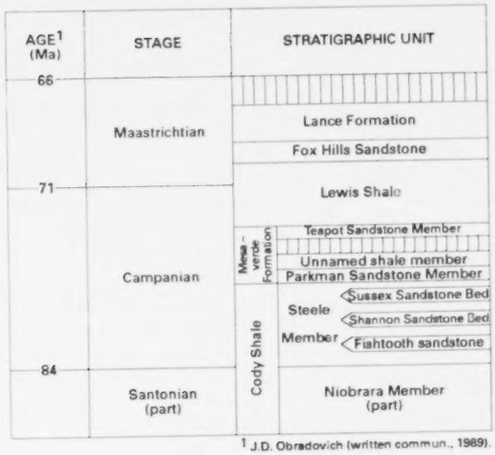

Figure 3. Stratigraphy of Upper Cretaceous rocks in the subsurface of the western part of the Powder River Basin.

alterations of outcrop and deeply buried sandstones were made by examination of both surface and subsurface samples.

Acknowledgments.—This report is a product of the U.S. Geological Survey Evolution of Sedimentary Basins Program. Gary L. Skipp was responsible for sample preparation and heavy-mineral separations. K.J. Esposito prepared specimens and generated X-ray diffractograms. April K. Vuletich determined the isotopic values for carbonate samples. E.A. Merewether graciously took the senior author to outcrops of the Shannon in the Salt Creek area and helped search for outcrops elsewhere in the basin. Greg Anderson of Home Petroleum Company, Denver, provided core (D568) from a producing reservoir sandstone in the Shannon for petrologic analyses.

RESEARCH DESIGN

The petrology of the Shannon Sandstone Beds was examined in samples taken from 10 cores (table 1) collected from drillholes along strike of the Shannon from Teapot Dome to the Wyoming-Montana State line (fig. 1). The Shannon in the cores is 12.3–39.0 m thick. Two cores (C221, D568) contain oil-producing intervals. Samples were also collected from outcrops of the Shannon at Salt Creek (fig. 1, locality SC) and from outcrops of the Shannon equivalent, the Groat Sandstone Bed of the Gammon Ferruginous Member of the Pierre Shale, in the eastern part of the basin (fig. 1, localities OC, HC, and HD). Samples of the Steele Member were collected from the cores for vitrinite reflectance studies so that the burial history of the Shannon could be assessed (Nuccio, 1990).

Petrographic thin sections were prepared from all sandstone samples collected from core and outcrop. The mineralogy of the Shannon was quantified (by volume) by counting 300 points each of selected thin sections.

Table 1. Outcrops and cores of the Shannon Sandstone Beds of the Steele Member of the Cody Shale and of the Groat Sandstone Bed of the Gammon Ferruginous Member of the Pierre Shale, Wyoming and Montana

[Locations shown by USGS designation (cores) or by two-letter code (outcrops) on fig. 1. Leaders (--) indicate not applicable]

Name	Oil field	USGS designation	Location	Depth (feet)	Depth (meters)
Felix and Scisson, Inc. 63 5 x 10	Teapot Dome	C221	Sec. 10, T. 38 N., R. 78 W.	245-366	74.7-111.6
Woods Petroleum Corp. 13-9 Pine Tree Unit	Wildcat	C652	Sec. 13, T. 41 N., R. 76 W.	10,790-10,840	3,289.6-3,304.9
Woods Petroleum Corp. No. 7-22	Pine Tree	C651	Sec. 7, T. 42 N., R. 75 W.	10,193-10,252	3,107.6-3,125.6
Diamond Shamrock Corp. No. 14-4	Hartzog Draw	A915	Sec. 4, T. 43 N., R. 74 W.	9,325-9,384	2,843-2,861
Southland Royalty Co. Van Irvine #3	Wildcat	A817	Sec. 22, T. 44 N., R. 77 W.	9,885-9,947	3,013.7-3,032.6
Woods Petroleum Corp. Knight State 16-1	Heldt Draw	A771	Sec. 16, T. 45 N., R. 76 W.	9,445-9,480	1,879.6-1,890.2
Davis Oil Company No. 10	Heldt Draw	B626	Sec. 36, T. 46 N., R. 76 W	9,365-9,418	2,855.2-2,871.3
Southland Royalty Co. Beaver Creek Federal No. 11	Wildcat	A729	Sec. 1, T. 48 N., R. 78 W.	8,580-8,618	1,615.9-2,627.4
Woods Petroleum Corp. Marton-Federal No. 20-1	Wildcat	A232	Sec. 20, T. 50 N., R. 80 W.	9,526-9,554	2,904.3-2,912.8
Home Petroleum Co. H-83 Culp Draw Unit	Hartzog Draw	D568	Sec. 5, T. 45 N.,R. 76 W.	9,495-9,544	2,894.8-2,909.8
Salt Creek (SC)	--	--	Sec. 15, T. 39 N., R. 79 W.	--	--
Owl Creek (OC)*	--	--	Sec. 26, T. 57 N., R. 2 E.	--	--
Horse Creek (HC)*	--	--	Sec. 24, T. 9 S., R. 61 E.	--	--
Hammond (HD)*	--	--	Sec. 26, T. 6 S., R. 56 E.	--	--

*Groat Sandstone Bed.

Each thin section was stained with alizarin red-S for calcite identification and with potassium cobaltinitrate for potassium feldspar identification. Polished thin sections of selected samples were also prepared for reflected light and scanning electron microscope (SEM) studies. Qualitative chemical analysis and elemental mapping were conducted on selected polished sections using the SEM energy-dispersive X-ray system (SEM-EDX). Heavy minerals (sp gr > 2.87) were separated from light minerals by gravity settling in bromoform; magnetic heavy minerals were separated from nonmagnetic heavy minerals using a hand magnet, and nonmagnetic heavy fractions were mounted on petrographic slides using canada balsam. Clay mineralogy was determined on the <2-μm fraction of sandstones using X-ray powder diffraction after air drying, saturation with ethylene glycol, and heat treatment at 550 °C. Examination of the cathodoluminescence of minerals under a Luminoscope enabled discrimination between detrital and authigenic phases that appeared homogeneous in transmitted light. A few typical sandstones containing one major carbonate phase were selected for isotope analyses. Stable isotope values ($\delta^{18}O$ and $\delta^{13}C$) were determined for siderite clasts and beds, detrital dolomite, and calcite.

DEPOSITIONAL ENVIRONMENT

The Shannon Sandstone Beds are considered to be a classic example of a mid-shelf sandstone (Tillman and Martinsen, 1984, 1987). Shannon sand ridges are interpreted to have formed at least 100–160 km from shore on a wide shelf along the western margin of the Western Interior Cretaceous seaway (Tillman and Martinsen, 1984, 1987). This interpretation is based primarily on a lack of shoreline facies and associated diagnostic trace fossils in the Shannon and on intertonguing of the Shannon both landward and seaward with marine shale. The position of the shoreline during Shannon deposition has been defined by ammonite zonation, mapping of strandlines, and K/Ar dating of bentonites (fig. 4) (Gill and Cobban, 1973). Shannon sand ridges are thought to have been deposited and shaped by storm currents flowing south-southwest (essentially parallel with the shoreline) across the shelf, transporting sediment from shoreline sands of the Eagle Sandstone about 320 km to the north in present-day southern Montana (Tillman and Martinsen, 1984). Gaynor and Swift (1988), however, proposed that the source for Shannon sand was "submarine erosion of the Montana shelf" by currents that produced a southward-extending sheet of muddy sand on the shelf. Shannon sand ridges were then built vertically on this thin layer of sediment by a complex interaction of storm, tidal, and longshore currents. The greatest accumulation of sand was in the Salt Creek anticline area (drillhole location C221, fig. 1), which may have been an actively growing paleostructural high around which sedimentation focused during Shannon deposition (Tillman and Martinsen, 1985).

According to the sea-level curves of Haq and others (1987), a eustatic rise occurred from about 83 to 81 Ma. Strandline reconstruction shows that at least one minor regression also occurred during this interval (Gill and Cobban, 1973, fig. 13). The Shannon was apparently deposited during this transgressive interval, about 81.5–81 Ma, by intermittent storm currents. The mechanism for concentrating sand into vertically accreting, coarsening-upward, linear ridges by storm-driven currents has been obscure, but recently Gaynor and Swift (1988) presented a complex model that explains the dynamics of ridge formation. They proposed that the Shannon is composed of beds and groups of beds that were deposited by storm-surge events; beds of a single event are separated by disconformities representing varying lengths of time. According to their model, the base of the Shannon, which is commonly marked by a zone of phosphatic pebbles, disconformably overlies the lower part of the Steele Member.

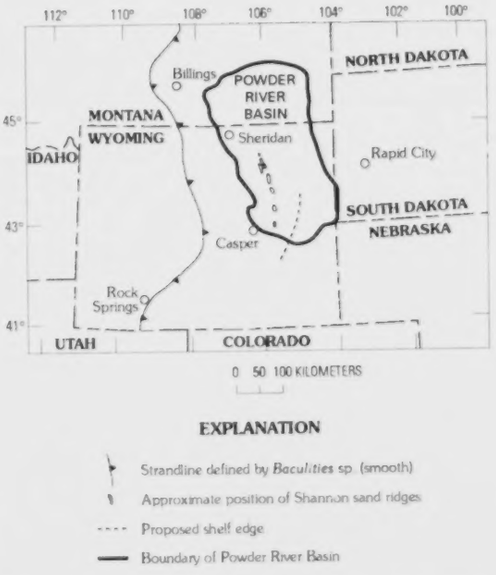

Figure 4. Inferred location of strandline defined by *Baculites sp.* (smooth) at the time of deposition of the Shannon Sandstone Beds. Generalized position of Shannon sand ridges and the edge of continental shelf are also shown. Compiled from Gill and Cobban (1973), Spearing (1976), and Seeling (1978).

The closest modern analogue to Shannon sand ridges on the Campanian shelf are mid-shelf sand bodies on the present-day Atlantic continental shelf off the east coast of the United States (Swift, 1985). Sizes of modern and ancient sand-ridge fields are similar. A typical cluster of Shannon sand ridges is 2.4 by 17.6 km at the Heldt Draw oil field, whereas a typical cluster of ridges on the modern continental shelf is 1.6–3.2 km by 16 km. Like Shannon sand ridges, modern ridges also rest on a transgressive surface. The formation of modern (and ancient) sand ridges, however, is a subject of debate. Some workers have proposed that modern sand ridges are storm- or tidal-built complexes that are presently forming on the shelf (Huthnance, 1982; Swift and others, 1986; Gaynor and Swift, 1988). Others contend that mid-shelf sand ridges are reworked barrier island or shoreface sequences. They argue for a multiple-stage origin for these linear sand bodies beginning with deposition as part of a shoreline sequence (accounting for their linearity), subsequent degrading and reworking during a transgression, and then, finally, reworking and aggrading by shelf currents into their present forms (Beaumont, 1984; Kiteley and Field, 1984; Stubblefield and others, 1984).

Some differences exist between modern and ancient ridges. For example, ancient sand ridges are generally farther from shore than modern ridges (Rice and Shurr, 1983). Some modern ridges (those closer to shore), unlike those of the Shannon, are oriented obliquely (5°–10°) to the coastline, an apparent anomaly that may be related to geotrophic storm current flow (Huthnance, 1982). Mid-shelf ridges, however, are oriented parallel with the coastline; thus, not all shelf ridges may form by the same process (Stubblefield and others, 1984). The Shannon sand ridges, unlike modern ridges on the Atlantic shelf, are restricted to a narrow band on the shelf. Modern sand ridges rest on a sandy shelf, whereas Shannon sand ridges extend upward from a muddy shelf and have a higher angle of repose. The angle of repose of a sediment has been interpreted to be directly related to grain size of shelf sediments; thus, deposition of the Shannon on a muddy rather than a sandy shelf may have resulted in the higher angle of repose for Shannon sand ridges (Swift and Rice, 1984).

Inferred water depth of 20–90 m during Shannon deposition is based on foraminiferal evidence from the Steele Member: most foraminifera are those characteristic of the inner shelf to shallow mid-shelf, and planktonic varieties are rare (Tillman and Martinsen, 1984); however, the Steele has an impoverished fauna characterized by low diversity of species. Lack of diversity may be due to factors such as low pH or abnormal salinity rather than to water depth. Interestingly, no foraminifera have been found in sideritic shale interbedded with sandstone of the Shannon.

Table 2. Correlation of depositional facies in Shannon Sandstone Beds as described herein with facies of the Shannon as defined by Tillman and Martinsen (1984)

This paper	Tillman and Martinsen (1984)
1a	Ridge-margin sandstone
1b	Central ridge sandstone
2	Inter-ridge sandstone
3	Bioturbated shelf sandstone
4	Shelf silty shale

Petrologic and sedimentologic data gathered during the present study indicate some characteristics of the Shannon that need to be addressed by the sand-ridge model: (1) abundant detrital dolomite grains and clasts; (2) large siderite clasts at the top and bottom of cross-bedded sandstone facies; (3) coal fragments and partings; (4) sideritic shales barren of foraminifera within the Shannon; (5) siderite and glauconite in the same bed; and (6) abrupt facies changes.

SEDIMENTOLOGY

The studied cores were divided into four descriptive facies: (1) fine- to medium-grained glauconitic sandstone containing locally common rip-up clasts and minimal burrowing; (2) very fine to fine grained, burrowed (< 75 percent burrowing) sandstone; (3) very fine to fine grained, bioturbated (> 75 percent burrowing) sandstone; and (4) dark-gray silty shale containing thin discontinuous sandstone laminae and rare to moderate burrowing. Correlation of these descriptive facies with genetic facies, as defined by Tillman and Martinsen (1984, 1985, 1987), is shown on table 2; facies in each core are described in the appendix.

Facies 1 has the best reservoir potential because of its relatively high porosity and permeability and larger grain size. It can be divided into two sub-facies: (1a) low- to medium-angle, trough crossbedded, glauconitic sandstone containing locally abundant shale and siderite rip-up clasts (fig. 5), and (1b) moderate-angle trough crossbedded to planar-laminated sandstone in which glauconite is less common and siderite clasts are rare. Abundant glauconite in facies 1a may produce a distinct green color. Facies 2 is characterized by discontinuous, horizontal, rippled sandstone and shale laminae that are truncated by horizontal, inclined, and (rarely) vertical burrows (fig. 6). Facies 3 lacks bedding and locally is mottled due to extensive burrowing. The only identified burrows are *Terebellina* or "donut" burrows (fig. 7), *Zoophycos*, and *Chondrites*. The diversity of burrowers is probably greater inasmuch as Tillman and Martinsen (1987) found 6–10 types of burrows, including *Terebellina*, *Teichichnus*, *Zoophycos*, *Chondrites*, and *Planolites*, in a detailed sedimentological study of the Shannon at the

Hartzog Draw field. Facies 4 is made up of laminated or massive shale and rare sandstone lenses containing minor burrowing and current ripples (fig. 8). The shale may be dolomitic, and bedded siderite is common (fig. 9). This facies is barren of foraminifera (Tillman and Martinsen, 1984).

The extensive burrowing and dominance of horizontal burrows in facies 2, 3, and 4 indicate a low to moderate sedimentation rate below wave base. *Terebellina* is thought to have lived in water at least 20 m deep (Chamberlain, 1978), but it, like *Chondrites*, can exist in a wide variety of depths from nearshore (about 10 m depth) to offshore (>60 m water depth) (Seilacher, 1978). The occurrence of organisms is controlled by many factors, only one of which is water depth; therefore, strict bathymetric interpretations based on trace fossil data are tenuous. Trace fossils give only a general indication of water depth—in the case of the Shannon, as has been interpreted as a mid-shelf setting. Other criteria must be used to better define the environment of deposition.

Figure 5. Abundant shale rip-up clasts characteristic of facies 1a in the Shannon Sandstone Beds; core A915 at 9,348 ft. Core is 4 in. in diameter.

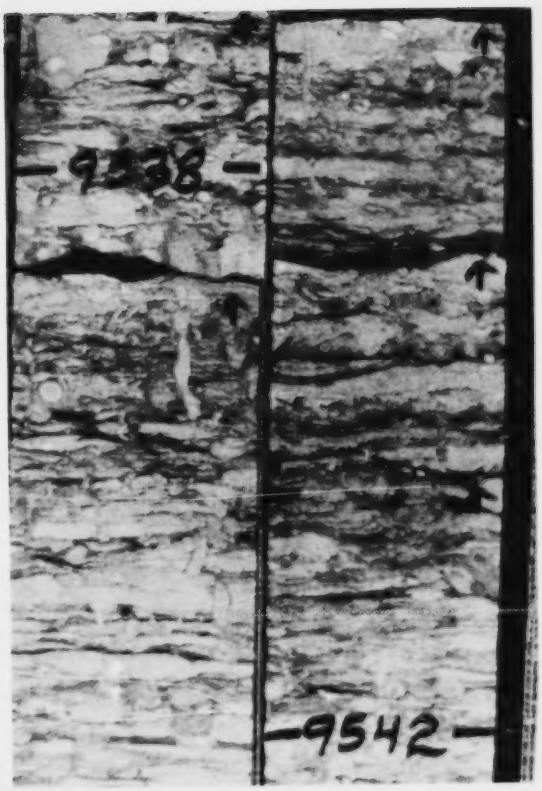

Figure 6. Burrowed sandstone characteristic of facies 2 of the Shannon Sandstone Beds; core D568. Core is 4 in. in diameter.

Coal fragments were observed in several cores, and apparent coal partings were found at the top of facies 2 in core A817 (fig. 10).

PETROLOGY

Sandstones from deeply buried cores (>2,500 m) are litharenites, whereas those from the outcrops and shallow cores (<100 m) are feldspathic litharenites according to Folk's (1974) classification (fig. 11). Shallowly buried and outcropping sandstones are plotted together, separate from deeply buried sandstones. Deeply buried sandstones contain less feldspar (fig. 11), mostly because of a loss of potassium feldspar (table 3). In Folk's classification, monocrystalline and polycrystalline quartz are grouped together, granitic and gneissic fragments are combined with feldspar, and chert is considered to be a rock fragment. Grain size of sandstones in the study area is from very fine to medium

Figure 7. *Terebellina* ("donut") burrows in bioturbated sandstone of facies 3 of the Shannon Sandstone Beds; core A232. Core is 4 in. in diameter.

Figure 8. Horizontally laminated black shale and interbedded sandstone with minor burrowing in facies 4 of the Shannon Sandstone Beds; core D568. Core is 4 in. in diameter.

grained, and the coarser sandstones are in the crossbedded and planar-laminated sandstone facies (facies 1a and 1b). Because these sandstones contain many rock fragments, grain size must be taken into account when interpreting sandstone classification.

Framework Mineralogy

Point-count analyses for 57 petrographic thin sections are shown in table 3. Major framework constituents are subangular to subrounded quartz, feldspar grains, and rock fragments. Monocrystalline quartz grains are generally free of inclusions and exhibit straight extinction. Polycrystalline quartz grains are probably plutonic in origin because they do not have sutured grain contacts. Plagioclase grains are untwinned or display simple twins and are of albite to andesine composition. The amount of plagioclase in shallow and deep samples is highly variable due to differing degrees of diagenesis. Potassium feldspar (microcline, orthoclase, perthite) is most abundant in outcrops and shallowly buried sandstones from the Teapot Dome oil field (fig. 1, locality C221) but has been replaced almost totally by calcite in sandstones from greater depths (fig. 12). Very fine grained sandstones generally contain more feldspar than coarser grained sandstones.

Major lithic fragments are chert, glauconite, dolomite, and siderite; minor varieties are igneous (plutonic and volcanic), sedimentary (argillaceous, phosphatic, and siltstone), and metamorphic (schist and phyllite). Angular to subangular chert is the most abundant rock fragment. Glauconite pellets (fig. 13) make up as much as 45 percent of rock fragments and 21 percent of total framework grains in some sandstones, especially in the crossbedded sandstone facies (1). In some beds they are so abundant as to give the sandstone a green color. Compaction has transformed some of the soft glauconite grains into pseudomatrix. Because glauconite pellets are composed mostly of interstratified glauconite-smectite, a diagenetic phase, their mineralogy is discussed later in the section on diagenetic alterations.

Figure 9. Bedded siderite (gold) and abundant glauconite (dark grains) in facies 4 of the Shannon Sandstone Beds overlying sandstone containing shale rip-up clasts in facies 1a; core A915 at 9,352.7 ft. Core is 4 in. in diameter.

Detrital monocrystalline (fig. 14) and polycrystalline (fig. 15) dolomite grains make up as much as 42 percent of rock fragments in fine-grained sandstones. The paucity of dolomite in fine- to medium-grained sandstones of the Shannon reflects the susceptibility of dolomite to abrasion in strong currents. Several criteria were used to determine whether single dolomite grains are detrital or authigenic: abraded surfaces on grains, positive size correlation with detrital quartz, clay rims on grains, composite grains, and round cores under euhedral overgrowths (table 4). A key test was examination of dolomite grains under a Luminoscope: detrital and authigenic parts of grains exhibited different degrees of cathodoluminescence so that some grains, which were apparently homogeneous under transmitted light, were seen to consist of rounded (detrital) cores within euhedral (authigenic) dolomite, ankerite, siderite, or other carbonate overgrowths (fig. 16). In addition, many dolomite grains have subrounded (interpreted to be abraded) surfaces coated by authigenic clay (fig. 17) and are sorted by size in the sandstones—that is, dolomite grains are just slightly smaller than associated quartz grains because of the higher density of dolomite.

Detrital siderite clasts (as much as 10 cm in diameter in the cores) make up as much as 22 percent of rock fragments in some sandstones of the Shannon (Ranganathan and Tye, 1986). Clasts are rounded to oblate and commonly are oriented parallel with bedding. They are associated with shale rip-up clasts and are most abundant at the top or base of facies 1a (fig. 18). The clasts are considered to be detrital because (1) they contain silt-size quartz and feldspar grains embedded in a micritic siderite matrix that is considerably finer grained than the sandstone in which the siderite clasts are found, and (2) bedding does not extend through the clasts. Siderite is present as lenses in facies 4 and as small rhombic crystals in facies 1 (see section on diagenetic alterations).

Minor framework constituents include muscovite, various heavy minerals (sp gr > 2.87), and organic matter such as fossil fragments and plant material. The most common heavy minerals noted in grain mounts are biotite, chlorite, dolomite, zircon, tourmaline, and apatite. Minor rutile, garnet, and hornblende were also observed. Biotite and chlorite compose more than half of most heavy-mineral fractions. Dolomite, which has a specific gravity of about 2.87, is discussed above. Zircons are colorless (rarely light pink) and well rounded; only a few euhedral grains were noted. Tourmaline is well rounded and gray brown to pink. Garnet is colorless or light pink and exhibits minor etch features. One or two rounded, dark-red rutile grains were observed in each sample. Elongate hornblende grains exhibiting distinct pleochroism (*Z*, yellow brown or olive green; *X*, green) and small extinction angles (< 15°) are locally common.

Opaque heavy minerals, mainly iron-titanium oxide minerals, are present in each sample.

Diagenetic Alterations

Diagenetic alterations are most pronounced in coarser sandstones of facies 1 in deep cores. Major authigenic minerals are siderite, pyrite, quartz, chlorite, glauconite-smectite, kaolinite, calcite, dolomite, ferroan carbonates, and albite. Minor authigenic minerals include apatite, hematite, barite, anhydrite, and potassium feldspar. Both intragranular and intergranular secondary porosity are well developed locally in the cross- and planar-bedded sandstones of facies 1. Framework grain alteration is mostly confined to feldspars. Potassium feldspar grains are relatively unaltered in shallow samples of all facies but have been replaced by calcite or albite in the deep samples. In very fine grained

Figure 10. Coal partings at the top of facies 2 of the Shannon Sandstone Beds; core A817 at 9,920.6 ft. Core is 4 in. in diameter.

sandstones of deep cores, however, potassium feldspars are unaltered, possibly because of the low permeability of the sandstones. Plagioclase exhibits varying degrees and types of alteration, from skeletalization in shallow samples to albitization in deeper samples.

Siderite

Small (<5 μm) rhombic siderite crystals commonly form a cement in sandstones containing siderite clasts. The siderite crystals formed early in the depositional history of the Shannon as indicated by their precipitation directly on the margins of framework grains and by their occurrence at grain contacts. They have been replaced locally by calcite cement (fig. 19). Qualitative chemical analyses made using the SEM–EDX system show that the siderite contains more calcium than most reported siderites. Some overgrowths on detrital dolomite grains have the composition of siderite (fig. 20).

Pyrite

Pyrite was most commonly found in samples that also contain organic matter and oil, notably in samples from core C221 (fig. 1). Different pyrite morphology of and textural relations between pyrite and other authigenic phases indicate that more than one generation of pyrite is present. Apparently late, framboidal pyrite (formed by bacterially mediated sulfate reduction after uplift) fills pores rimmed by quartz overgrowths (fig. 21), pyrite euhedra are intergrown with authigenic chlorite (fig. 22), and micron-size (early?) euhedral pyrite is in glauconite grains and within patches of calcite cement. SEM-EDX spectra of pyrite euhedra from samples from the Teapot Dome oil field (fig. 1, locality C221) indicate that the pyrite lacks sulfur; the crystals are probably iron oxide pseudomorphs after pyrite (fig. 23).

Quartz

Detrital quartz grains in facies 1 from deep cores are commonly cemented by syntaxial quartz overgrowths that are coated with oil (fig. 24) and locally etched (fig. 25) in reservoir sandstones. Quartz overgrowths generally overlie chlorite rims, but authigenic chlorite and quartz are intergrown in some samples (fig. 26).

Chlorite

Chlorite was found in relatively deep cores (>2,500 m) but not in outcrop or shallow core samples. It is most commonly a coating or alteration product (?) of glauconite grains, but it also rims framework grains. Grain coatings of chlorite lie underneath albite and quartz overgrowths (fig. 27); chlorite-lined pores are commonly filled with (later) calcite cement. In some samples, chlorite and quartz overgrowths appear to have precipitated at the same time (see fig. 26).

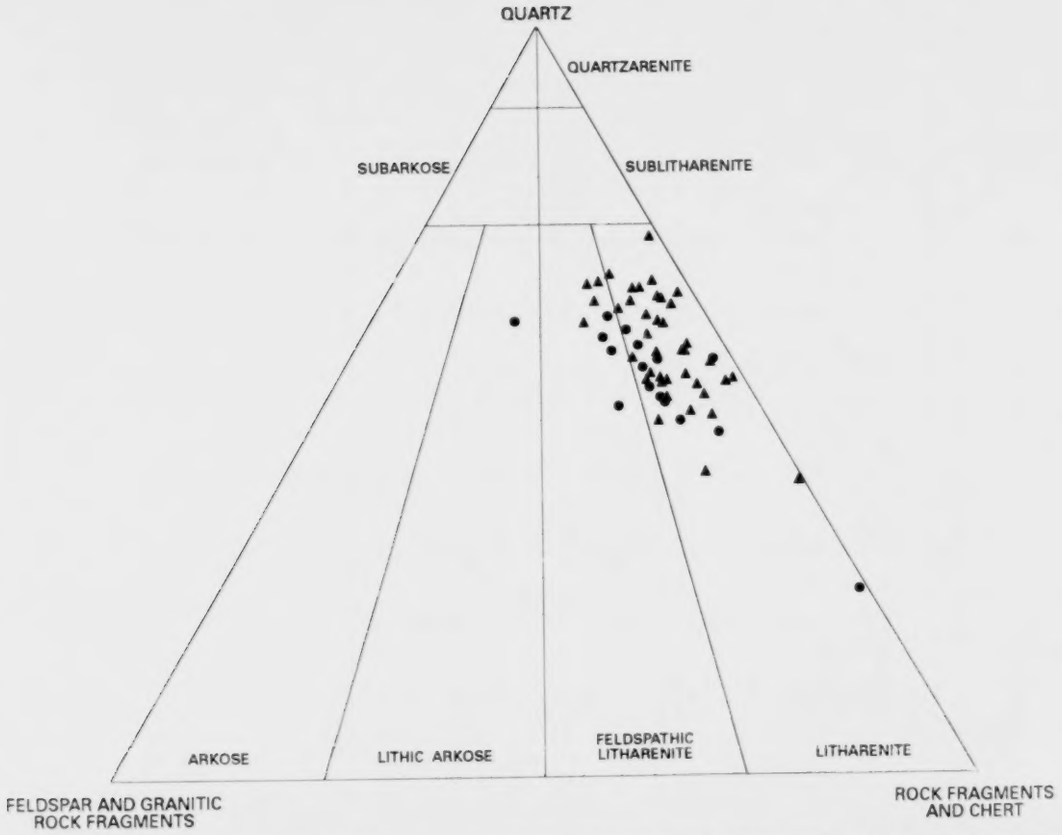

Figure 11. Composition (as determined from point counts) of sandstones from the Shannon and Groat Sandstone Beds. Circles indicate outcrop and shallow samples (< 150 m depth); triangles indicate deep samples (> 2,500 m depth). Sandstone classification diagram from Folk (1974).

Calcite

Calcite that precipitated before significant compaction is found between muscovite plates and as a poikilotopic cement in outcrop and near-surface sandstones. In sandstones that were cemented by early calcite, chlorite and quartz overgrowths are rare, grain contacts are tangential, and skeletal plagioclase grains are within calcite-cemented areas (as, for example, in samples C221–253, –256, –262). Ferroan calcite cement (possibly a replacement of earlier carbonate cement) is found in the Groat Sandstone Bed. In deeply buried sandstones, calcite cementation followed chlorite and quartz overgrowth precipitation. This later calcite cement partly to completely replaces and (or) infills most potassium feldspar in fine- and medium-grained sandstones (fig. 28). Complete replacement is inferred by a spectrum of replacement textures ranging from potassium feldspar partly replaced by calcite to grain-sized patches of calcite devoid of potassium feldspar. In many samples, patches of calcite cement in optical continuity are evidence of later calcite dissolution.

Glauconite-Smectite

The term "glauconite" has had a dual meaning for many years. Glauconite is the mineralogical name for a specific iron-rich mica that is distinguished from celadonite and other micas by chemical composition, d(060) value, and infrared spectral characteristics (Bailey, 1980; Bailey and others, 1984). A mixed-layer mineral composed of interstratified glauconite and smectite layers is termed interstratified glauconite-smectite. The identification of glauconite as a mineral is independent of

Table 3. Point counts of selected thin sections of the Shannon Sandstone Beds and Groat Sandstone Bed, Powder River Basin

[Core and outcrop localities shown on fig. 1 and given in table 1. Abbreviations: Rk Frag: rock fragments; og, overgrowth; Other: anhydrite, barite, carbonate overgrowths, potassium feldspar overgrowths]

Sample	ϕ	Qtz	K-feldspar	Plag	Rk Frag	Glauconite	Dolomite	Opaques	Musc	Biotite	Clay	Calcite	Qtz og	Albite og	Pyrite	Other	Organics	Void
									A771									
9,449.5	2.10	115	0	6	64	24	0	0	0	0	23	4	63	1	0	0	0	0
9,453	2.10	148	0	13	54	27	4	0	1	1	25	2	18	1	0	0	0	6
9,456	2.00	168	0	3	53	9	0	0	0	0	39	4	17	0	0	0	1	6
9,457	2.00	137	0	4	50	22	3	0	0	0	34	3	26	1	0	0	0	2
9,459.5	2.30	135	0	9	55	13	0	0	0	0	25	14	30	2	0	0	0	17
9,467.5		115	0	7	41	7	22	1	2	2	87	5	11	0	0	0	0	0
9,475		113	1	11	41	6	12	0	0	2	101	5	7	0	1	0	0	0
									A232									
9,527	3.20	112	2	21	34	31	12	0	0	1	75	5	5	1	0	0	1	0
9,540	3.30	110	6	4	30	19	18	0	0	0	105	3	0	0	2	3	0	0
9,548	3.25	128	4	8	54	29	3	2	1	1	42	23	5	0	0	0	0	0
									C652									
10,800	3.00	118	1	20	50	12	24	1	0	2	32	4	27	7	0	1	1	0
10,807	3.00	102	0	21	51	17	18	1	0	0	23	0	62	4	0	1	0	0
10,818	3.25	118	2	16	55	7	12	0	1	0	40	7	33	9	1	0	0	0
10,828	3.75	95	2	15	48	1	36	1	2	8	73	1	15	2	0	0	1	0
									A729									
8,580	2.50	87	0	24	56	46	3	0	0	5	56	1	20	1	0	1	0	0
8,587.5	2.25	139	0	22	55	7	0	0	1	0	22	7	43	2	0	0	0	2
8,588	2.20	143	0	10	68	3	0	0	1	0	15	7	47	5	0	0	0	1
8,599.5	2.50	142	0	25	32	7	10	1	0	1	6	0	47	5	0	0	2	0
8,614	1.90	138	0	16	56	15	0	0	0	0	22	6	45	2	0	1	0	0
									C221									
253.8	2.00	123	4	2	59	35	0	0	0	0	2	75	0	0	0	0	0	0
269.2	2.50	127	12	18	45	16	0	0	1	0	11	0	4	0	1	0	0	65
300	3.00	117	13	8	38	14	15	1	1	1	77	1	0	0	1	0	1	12
334	2.75	141	8	26	64	7	4	2	0	1	4	4	0	0	0	0	0	39
337.2	3.00	131	15	8	46	15	6	0	1	2	32	0	0	0	0	0	2	42
353	2.75	106	10	14	53	14	15	1	2	1	46	4	4	0	6	0	0	25
358	3.00	109	17	8	43	13	22	0	0	2	63	2	0	0	0	2	0	21
362	3.00	109	9	9	42	7	22	0	0	3	94	0	0	0	0	0	0	5
365	3.00	97	13	9	47	6	25	0	2	7	90	1	0	0	2	0	0	1

Table 3. Continued

Sample	ϕ	Qtz	K-feldspar	Plag	Rk Frag	Glauconite	Dolomite	Opaques	Musc	Biotite	Clay	Calcite	Qtz og	Albite og	Pyrite	Other	Organics	Void
D568																		
9,507	2.00	110	1	4	74	20	1	0	0	11	80	0	0	0	0	0	0	0
9,509.8	2.25	121	0	12	60	18	3	0	0	1	44	2	26	0	0	0	0	13
9,512	2.25	114	0	9	56	20	0	0	2	0	26	1	44	1	0	0	1	22
9,513.5	0.75	87	0	1	128	5	0	0	0	0	57	4	0	0	0	0	17	0
9,515.5	1.75	100	0	12	52	28	1	1	0	1	73	0	30	0	0	0	0	3
9,526.5	3.50	83	6	7	4	3	23	0	1	1	93	43	0	0	6	0	13	0
9,535	3.25	117	3	12	63	7	18	0	0	1	44	2	26	0	0	0	0	13
9,542	3.25	125	3	4	40	7	20	0	0	0	83	2	9	0	0	0	7	0
C651																		
10,198	3.00	108	3	10	52	20	21	0	0	0	57	6	14	1	0	0	2	0
10,202	2.50	117	0	16	69	42	1	0	0	1	19	6	18	3	1	0	1	0
10,210	2.00	125	0	12	53	13	5	0	0	0	42	3	37	1	0	0	0	9
10,227	1.60	113	0	3	75	23	0	0	0	0	38	2	35	0	0	0	0	12
10,230	2.25	111	1	13	32	5	4	0	0	0	103	3	26	1	0	0	0	1
10,234	2.25	136	0	17	49	11	2	1	0	0	48	0	28	1	0	0	0	9
10,248	3.25	120	0	22	59	15	11	0	0	3	40	7	21	1	0	0	1	0
A817																		
9,899.6	2.75	126	0	31	36	12	4	0	0	1	16	3	30	5	0	0	8	0
9,907	2.50	118	0	25	77	16	2	0	1	1	5	8	31	4	0	0	0	11
9,911.4	2.50	121	0	23	23	23	1	0	0	1	41	2	26	3	0	0	0	6
9,917.6	3.00	139	0	20	59	16	3	0	0	2	25	10	11	6	0	0	3	5
9,931	3.50	113	15	16	60	5	31	1	0	0	43	7	10	0	0	0	3	0
B626																		
9,391	2.50	128	0	24	52	28	13	0	1	0	15	7	26	1	0	0	1	4
9,404.5	2.50	105	2	21	60	12	0	1	1	0	1	93	2	1	1	0	0	0
*HORSE CREEK (HC)																		
3	3.00	103	20	3	64	18	11	1	0	1	5	41	0	0	0	4	0	30
5	1.50	52	3	0	104	51	2	0	0	0	7	79	0	0	0	0	2	0
6	2.75	89	10	4	61	24	8	1	0	1	2	97	0	0	0	3	0	0
*HAMMOND (HD)																		
1	2.75	97	13	7	52	4	6	0	0	1	3	116	0	0	0	1	0	0
SALT CREEK (SC)																		
2	2.75	133	12	16	49	2	8	0	2	0	9	19	0	0	0	4	0	54
4	2.50	110	18	3	46	3	0	0	0	1	5	114	0	0	0	0	0	0
6	2.75	124	16	26	77	10	0	0	0	1	8	1	0	0	0	0	0	37

*Groat Sandstone Bed.

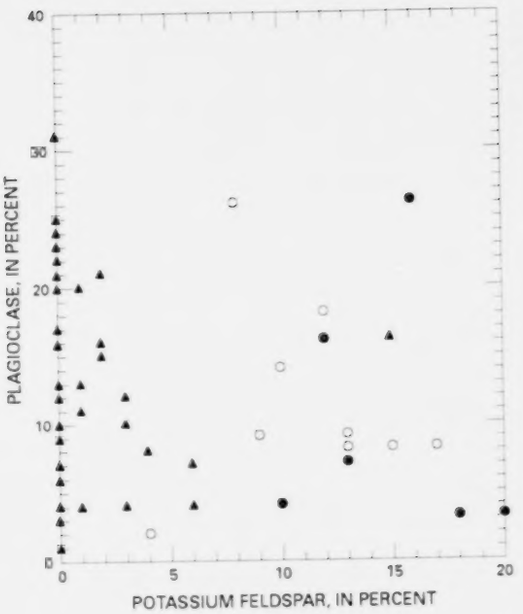

Figure 12. Plot of plagioclase versus potassium feldspar abundance (percent of normalized framework grains) as derived from point counts of petrographic thin sections of the Shannon and Groat Sandstone Beds. Solid circles indicate outcrop samples; open circles indicate shallow core samples (< 120 m depth); solid circles indicate deep core samples (> 2,500 m depth).

its mode of origin. Glauconite also has historically been used as a morphological term for sand-size greenish grains that are commonly thought to be fossil fecal pellets (McRae, 1972). When used as a rock term in this manner, it does not imply a particular mineralogical composition, though glauconite pellets commonly are rich in the mineral glauconite. Odin and Fullagar (1988) attempted to clarify the terminology by introducing the term "glaucony" as a facies term for sediments containing the green pellets, and "glauconitic mineral" for the minerals that make up such sediments. We use the term "glauconite" as a morphological or rock term, and we use the specific mineralogical term "glauconite-smectite" for the interstratified mineral.

Glauconite pellets in the Shannon are composed dominantly of interstratified glauconite-smectite having a high proportion of smectite layers in shallow samples and a low proportion of smectite layers in the deeper samples. A d(060) of 1.52 Å confirms that the phase is glauconite-smectite. The proportion of smectite layers in the glauconite-smectite from the shallow samples (75–112 m) is from 40 to 60 percent. Deeper samples (2,640–3,333 m) have expandabilities of 10–20 percent. Well-developed lamellae of glauconite in the deeper samples, as seen under the SEM (fig. 29), are characteristic of older, highly diagenetically evolved glauconite (Odin and Morton, 1988). Both the shallow and deep samples commonly contain discrete mica and discrete chlorite (fig. 30).

Albite

Albitized plagioclase and potassium feldspar grains and albite overgrowths on plagioclase and on albitized potassium feldspar grains were found in deep core samples (> 2,500 m). Albitized potassium feldspar grains are similar in appearance to "chessboard" albite (fig. 31) as described by Walker (1984); however, SEM-EDX analysis did not detect any residual potassium in the albite, but perhaps the sensitivity of the instrument was not high enough or replacement of the potassium feldspar by albite was complete. Some potassium feldspar grains have been both partly albitized and partly calcitized.

Minor Authigenic Phases

Apatite cement surrounds framework grains in sample D568–9,513.5, which is a poorly sorted sandstone that contains large (as much as 10 μm) foraminiferal, plant, and phosphatic rock fragments. Apatite cement around sedimentary fragments that have an apatite matrix suggests that apatite in the detrital fragments was dissolved and reprecipitated in the Shannon. Euhedral potassium feldspar overgrowths are rare in the Shannon but were noted in samples C221–340 and C221–353 and in the Groat Sandstone Bed underlying ferroan calcite cement. Small patches of barite and anhydrite cement were observed in only a few thin sections.

Small (< 5 μm) euhedral dolomite grains in very fine grained sandstones may be authigenic. Ferroan dolomite overgrowths are locally common on detrital dolomite grains (fig. 32), particularly in cores C652 and A771.

Secondary Porosity

In near-surface and surface sandstones, moldic porosity has resulted from dissolution of plagioclase (fig. 33). In places, ragged edges of framework grains and patches of calcite cement in voids imply the dissolution of calcite cement. Intragranular secondary microporosity has resulted from partial dissolution of chert grains.

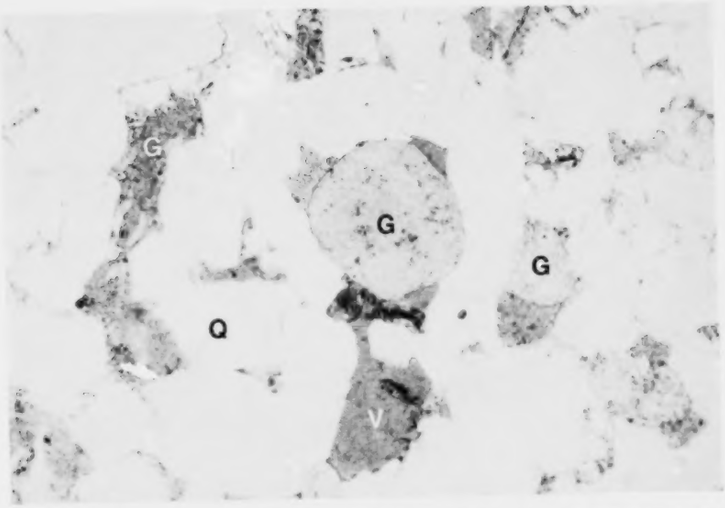

Figure 13. Photomicrograph of detrital glauconite grains (G) and quartz (Q). V, void filled with blue-dyed epoxy. Core A771 at 9,457 ft. Plane-polarized light; field length 1.2 mm.

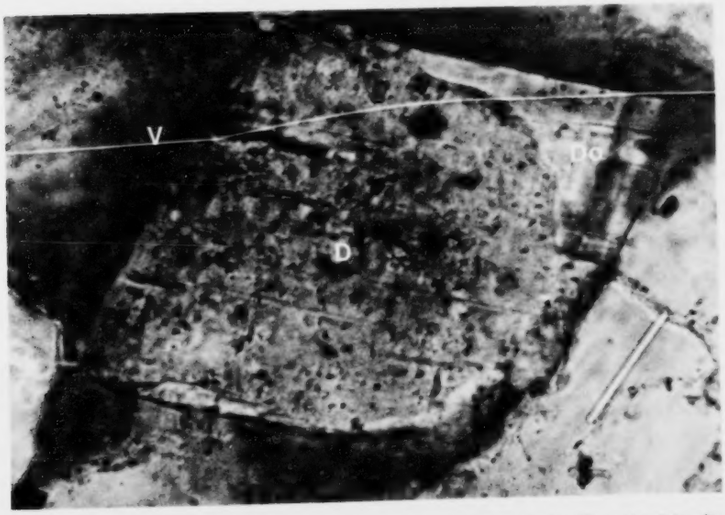

Figure 14. Photomicrograph of rounded detrital dolomite grain (D) with dolomite overgrowth (Do). V, void. Core C221 at 334 ft. Plane-polarized light; field length 0.34 mm.

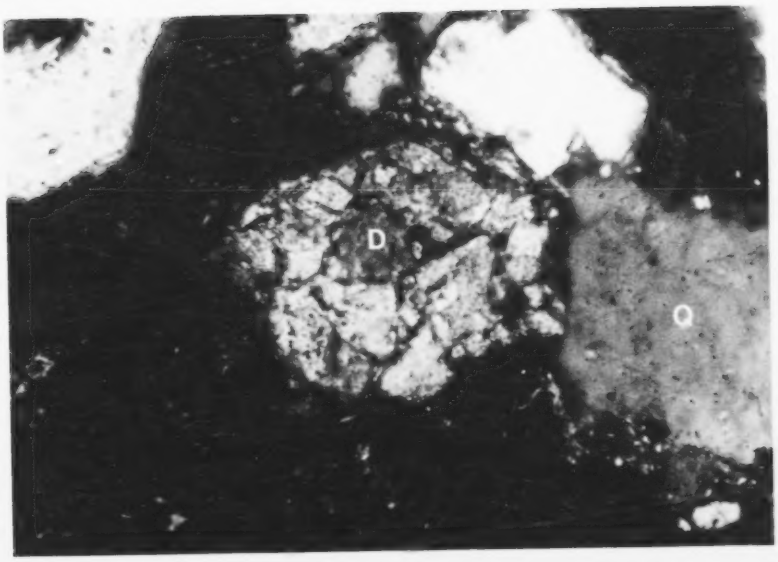

Figure 15. Photomicrograph of detrital polycrystalline dolomite clast (D) and quartz (Q). Core C221 at 276 ft. Crossed nicols; field length 0.43 mm.

Figure 16. Cathodoluminescence micrograph showing (1) detrital dolomite grain (red) and calcite overgrowth (orange); (2) calcite grain (orange) with dolomite overgrowth (red); and (3) dolomite grain (red) with dolomite overgrowth (red). Core A771 at 9,475 ft. Field length 1.5 mm.

Table 4. Identification criteria for detrital dolomite

Grains have abraded surfaces
Positive size correlation with detrital quartz
Clay rims on grains
Composite grains
Round cores under euhedral overgrowths as revealed by:
Cathodoluminescence
X-ray fluorescence elemental mapping

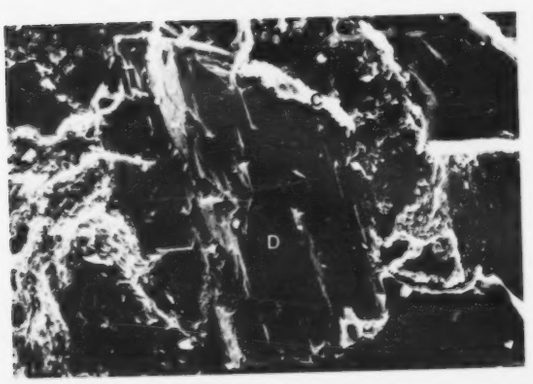

Figure 17. Scanning electron micrograph of detrital dolomite grain (D) and clay rim (C). Core C652 at 10,807 ft. Field length 0.15 mm.

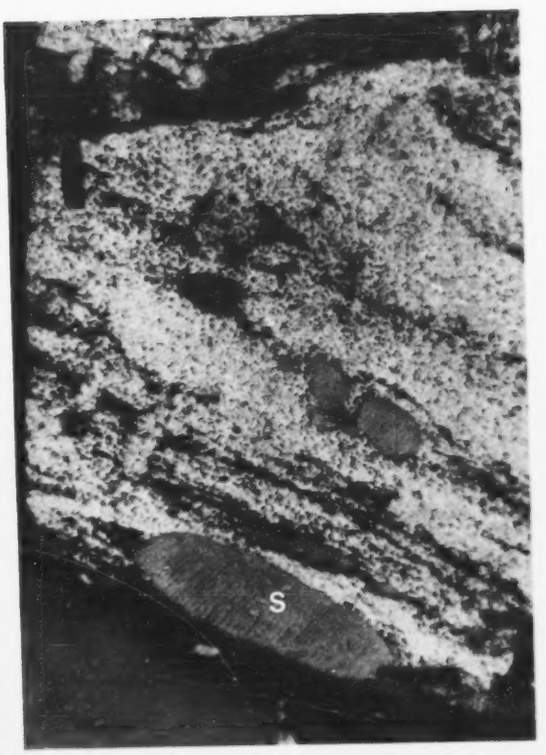

Figure 18. Golden-brown detrital siderite clasts (S) lying parallel with bedding at base of facies 1a of the Shannon Sandstone Beds; dark grains are glauconite. Core C221 at 253.8 ft. Core is 4 in. in diameter.

Minor etching of quartz grains was noted in some oil-bearing sandstones (see fig. 25).

Oil

During SEM analysis, oil droplets were noted on the surfaces of quartz overgrowths that project into secondary pores (see fig. 24). Oil was also observed on quartz overgrowths in thin section (fig. 34).

ISOTOPY

Procedure

The stable isotope geochemistry of minerals can give valuable information regarding the chemistry and temperature of the pore waters from which the minerals precipitated and the chemical process by which the isotopes were fractionated. Samples containing a high percentage of one carbonate phase (such as calcite, siderite, or dolomite) were selected for $\delta^{13}C$ and $\delta^{18}O$ analyses. Samples were pulverized, isolated under a vacuum, and then reacted with 100 percent phosphoric acid resulting in the evolution of CO_2 (McCrea, 1950). In samples containing calcite and siderite, the CO_2 evolved during the first 3 hours was assumed to be from calcite; the CO_2 evolved over the next 93 hours was assumed to be from siderite. Two samples containing only dolomite as a carbonate phase were also analyzed. Isotopic data are shown on table 5.

Calcite

Two typical calcite-bearing sandstone samples of the Shannon were selected: one from Salt Creek (sample SC–4) contains 38 percent calcite by volume, and the

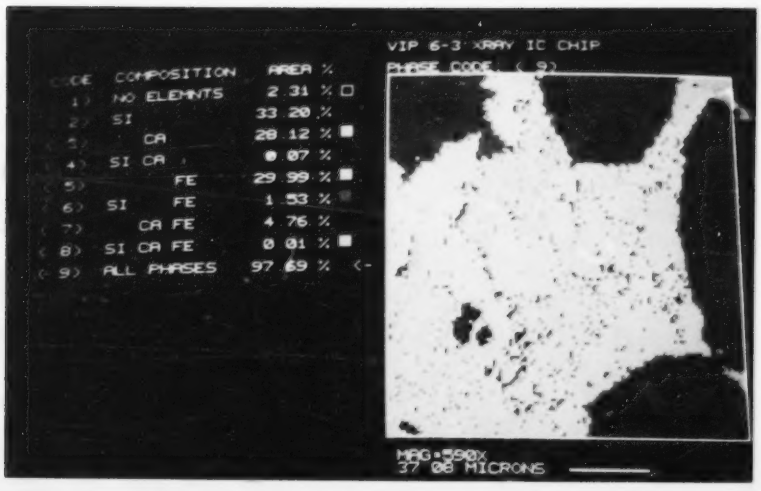
VIP 6-3 XRAY IC CHIP
PHASE CODE (9)
CODE COMPOSITION AREA %
1) NO ELEMNTS 2.31 %
2) SI 33.20 %
3) CA 20.12 %
4) SI CA 0.07 %
5) FE 29.99 %
6) SI FE 1.53 %
7) CA FE 4.76 %
8) SI CA FE 0.01 %
9) ALL PHASES 97.69 %
MAG=500X
37.00 MICRONS

Figure 19. Scanning electron X-ray fluorescence micrograph showing the relation between authigenic siderite (gray) and calcite (pink) in a pore; quartz grains are purple. Note correlation between elemental composition and color. Core A771 at 9,461.5 ft.

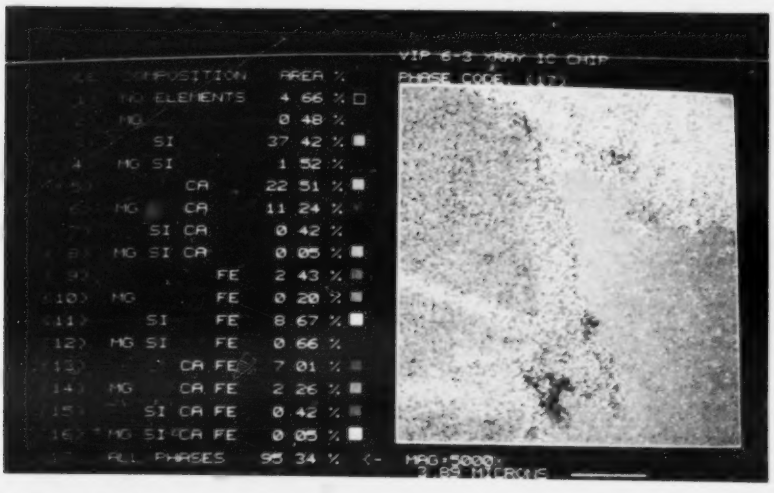
VIP 6-3 XRAY IC CHIP
CODE COMPOSITION AREA %
1) NO ELEMENTS 4.66 %
2) MG 0.48 %
3) SI 37.42 %
4) MG SI 1.52 %
5) CA 22.51 %
6) MG CA 11.24 %
7) SI CA 0.42 %
8) MG SI CA 0.05 %
9) FE 2.43 %
10) MG FE 0.20 %
11) SI FE 8.67 %
12) MG SI FE 0.66 %
13) CA FE 7.01 %
14) MG CA FE 2.26 %
15) SI CA FE 0.42 %
16) MG SI CA FE 0.05 %
ALL PHASES 95.34 %
MAG=5000X

Figure 20. Scanning electron X-ray fluorescence micrograph showing siderite overgrowth (red) on detrital dolomite grain (blue); siderite also fills fracture in dolomite grain. V, void (pink). Core A771 at 9,461.5 ft.

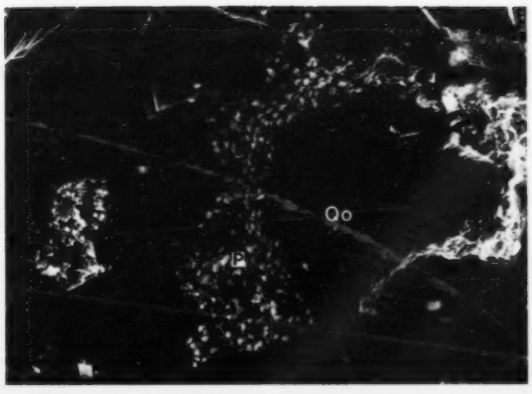

Figure 21. Scanning electron micrograph of framboidal pyrite (P) in pore lined by quartz overgrowths (Qo). Core C652 at 10,800 ft. Field length 90 mm.

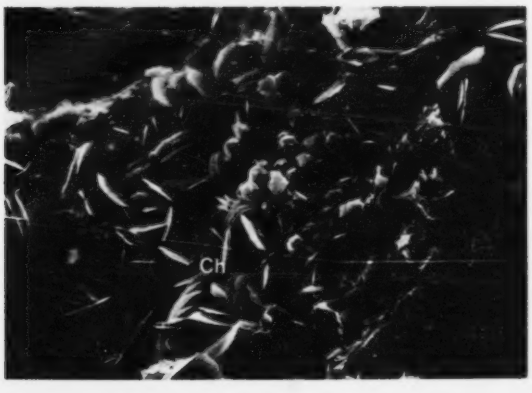

Figure 22. Scanning electron micrograph of authigenic pyrite euhedra (P) and authigenic chlorite (Ch). Core B626 at 9,391 ft. Field length 30 mm.

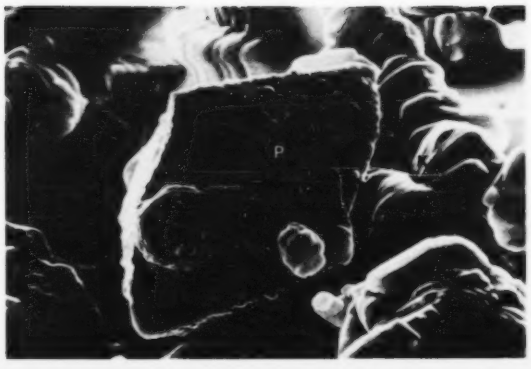

Figure 23. Scanning electron micrograph of iron oxide pseudomorph (octahedral crystal contains iron but no sulfur) after pyrite (P); vermicular kaolinite (K) surrounds the pseudomorph. Core C221 at 334 ft. Field length 25 mm.

Figure 24. Scanning electron micrograph of quartz overgrowth coated with oil (raised protuberances are oil droplets). Core D568 at 9,509.6 ft. Field length 28 mm.

other from the Teapot Dome oil field (sample C221–253.8) contains 25 percent calcite by volume. In both sandstones, framework grains are solidly cemented with poikilotopic calcite. Neither sandstone displays significant diagenetic alteration, and high minus-cement porosity values for both indicate that calcite was precipitated during early diagenesis. The light $\delta^{13}C$ values (-10.61 and -12.72 per mil) of calcite (inferred to have precipitated at ambient temperatures) probably resulted from the mixing of CO_2 derived from the metabolism of organic matter (about -25 per mil), CO_2 derived from the atmosphere (about -7 per mil), and (or) CO_2 derived from dissolution of marine carbonate ($\delta^{13}C$ of about 0 per mil) (Carothers and Kharaka, 1980). The relatively light $\delta^{18}O$ values (-12.00 and -12.25 per mil) suggest meteoric water influence and (or) precipitation of calcite in a closed system in which the $\delta^{18}O$ of the water became increasingly lighter as oxygen-bearing minerals precipitated (Longstaffe, 1988).

Dolomite

Two sandstone samples, C221–300 (about 5 percent dolomite by volume) and C652–10,828 (12 percent dolomite by volume), that contain detrital dolomite and no other carbonate minerals were chosen for isotopic analyses. The dolomite is present as monocrystalline and polycrystalline grains. Dolomite overgrowths compose a very small percentage of the total volume of dolomite. The isotopic values ($\delta^{18}O$, -6.10 and -4.64 per mil; $\delta^{13}C$, -2.65 and -4.20 per mil) are slightly

Figure 25. Scanning electron micrograph of etch pits in quartz overgrowth from reservoir sandstone. Core D568 at 9,509.8 ft. Field length 26 mm.

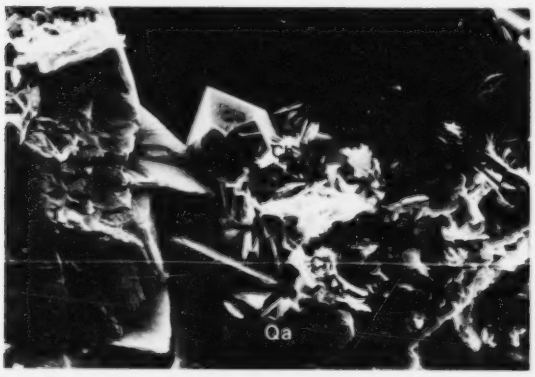

Figure 26. Scanning electron micrograph of intergrowth of authigenic quartz (Qa) and chlorite (Ch). Core A729 at 8,580 ft. Field length 60 mm.

lower than values typical of carbonate-platform dolomites that formed by the replacement of a pre-existing calcium carbonate phase and, in the process, preserved isotopic values of the early carbonate (Land, 1980). Lower isotope values may be due to incorporation of light carbon derived from oxidation of organic matter.

Siderite

Isotopic analysis of detrital siderite clasts collected from cores yields relatively light $\delta^{13}C$ values (-12.95 to -14.45 per mil) that suggest the concretions formed during sulfate reduction rather than methanogenesis, a process characterized by heavy $\delta^{13}C$ from about -4 to +11 per mil (Curtis and others, 1986). $\delta^{18}O$ values (-2.61 and -2.49 per mil) are slighter lighter than seawater values, possibly due to diagenetic processes. The $\delta^{13}C$ (-7.05 and -5.92 per mil) and $\delta^{18}O$ (-2.25 and -0.85 per mil) values for two samples of bedded siderite are somewhat heavier than comparable values for siderite clasts. The $\delta^{18}O$ values are fairly typical of seawater—the lower value may be slightly evolved owing to diagenesis—and the $\delta^{13}C$ values may indicate minor input of some heavy CO_2 derived from methanogenesis. More definitive interpretations cannot be made using isotopic values for only two samples.

DISCUSSION

Provenance

Sand deposited as the Shannon may have been reworked from shoreline sands (see fig. 4) of the Eagle Sandstone (Gautier, 1981a). Paleogeographic reconstructions indicate that the source area for the Eagle and therefore the Shannon was in western Wyoming and Montana (Shurr, 1984). The abundance of chert suggests that source rocks were predominantly sedimentary and included minor plutonic, metamorphic, and volcanic components; however, some labile minerals and rock fragments may have been lost by attrition resulting from the great distance (>300 km) of the Shannon from source areas and extensive reworking by shelf currents.

The relatively light carbon isotopic values for detrital siderite clasts in the Shannon indicate that siderite did not form during methanogenesis (Curtis and others, 1986). In contrast, heavy values, averaging +5 per mil, for siderite in the Shannon Sandstone Member of the Gammon Shale in Montana and southwestern North Dakota are characteristic of fractionation during methanogenesis (Gautier, 1981b). Light $\delta^{13}C$ values suggest that the siderite clasts formed in lagoonal or estuarine environments, both of which are characterized by iron concretions and where isotopically light CO_2 is available. The siderite was then ripped up, transported, and redeposited by currents on the shelf. The large size of many clasts precludes long-distance transport.

Origin of Glauconite

Studies of glauconite in Holocene sediments suggest that glauconite formation involves the alteration of a substrate, such as fecal pellets or foraminiferal tests, in contact with seawater at depths between 60 and 500 m (Odin and Fullagar, 1988; Odin and Morton, 1988). Although glauconite cannot be used as a precise water-depth indicator, its presence constrains the depth of

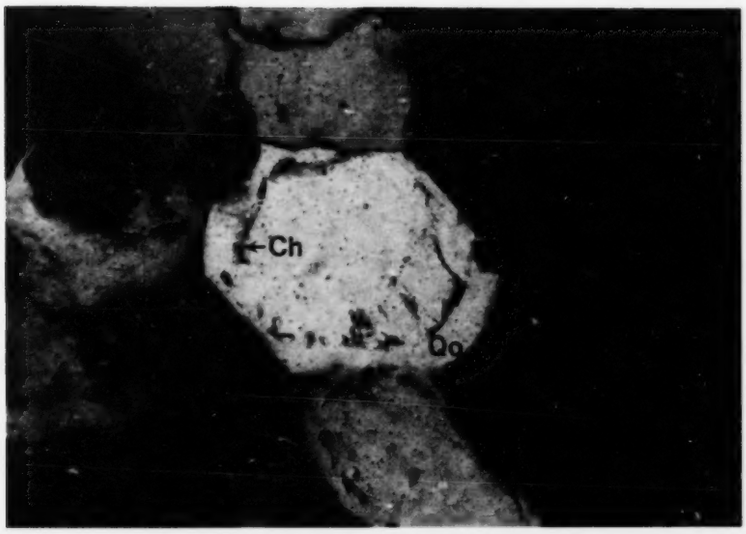

Figure 27. Photomicrograph of authigenic chlorite rim (Ch) under quartz overgrowth (Qo). Core A771 at 9,453 ft. Crossed nicols; field length 0.55 mm.

formation to below wave base on the continental shelf. Glauconite forms in an environment where winnowing exceeds detrital input. Thus, transgression produces an environment that is highly favorable for glauconite formation, and glauconite is commonly found at the base of a transgressive sequence (Odin and Fullagar, 1988).

Origin of Dolomite

Detrital dolomite is a common constituent of many Western Interior Cretaceous sandstones (Sabins, 1962; Young and Doig, 1986); however, in a previous petrologic study (Ranganathan and Tye, 1986), all dolomite in the Shannon was considered to be authigenic. The most probable sources for the detrital dolomite are erosion of syndepositional dolomite from shallow tidal flats by transgression of the Cretaceous sea and weathering of dolomite-bearing rocks in the source area.

Supratidal crusts may have provided some dolomite to the Shannon. Sabins (1962) suggested that monocrystalline dolomite grains ("primary" dolomite) in marine Cretaceous sandstones formed nearby within the depositional basin and were reworked locally into the sandstones. He did not, however, suggest a mechanism for dolomite precipitation, an important point because dolomite is not known to precipitate directly from normal marine seawater. The only modern environment in which dolomite precipitation at ambient temperatures has been documented is a supratidal setting in which the Mg/Ca ratio is elevated due to evaporation of seawater (Hardie, 1987); however, dolomite that forms in a tidal environment tends to be micron size and not sand size, as are most grains found in the Shannon.

Several Paleozoic formations, such as the Ordovician Bighorn Dolomite, in the source area of the Shannon may have provided sand-size dolomite grains. Modern stream sediments in central Texas contain abundant detrital dolomite that has weathered from the Ellenburger Group (Ordovician); however, dolomite decreases greatly in abundance downstream when streams reach more abrasive marginal- and open-marine environments (Amsbury, 1962). Likewise, carbonate fragments may have been more abundant in the source area than present-day amounts in the Eagle and Shannon indicate.

To minimize abrasion, dolomite grains were probably transported in fast-moving streams and moved rapidly to the shoreline and out onto the shelf. The Campanian shoreline along the western margin of the seaway was formed by the Eagle Sandstone, which contains 5–10 percent (by volume) detrital dolomite as polycrystalline and mostly monocrystalline sand-size grains (Gautier, 1981a). The sizes and textures of dolomite grains in the two formations are similar; thus, some detrital dolomite was probably transported by longshore and storm currents from the Eagle shoreline onto the shelf where it was incorporated along with other clastic grains into Shannon sand ridges. In this study, the

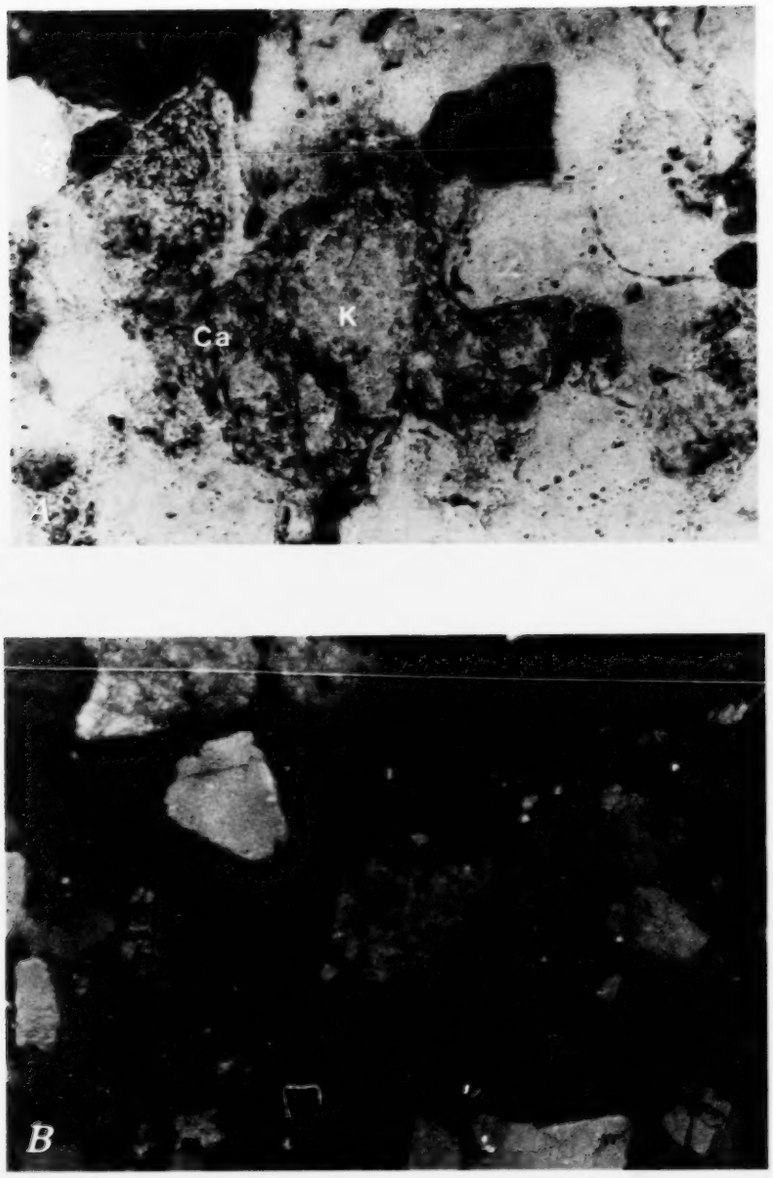

Figure 28. Diagenesis of potassium feldspar. *A*, Photomicrograph showing partial replacement of potassium feldspar (K) by calcite (Ca). Core A232 at 9,527 ft. Crossed nicols; field length 0.5 mm. *B*, Cathodoluminescence micrograph showing replacement of potassium feldspar (blue) by calcite (orange). Core A771 at 9,475 ft. Field length 0.4 mm. Exposure time 33 seconds; 20 kV.

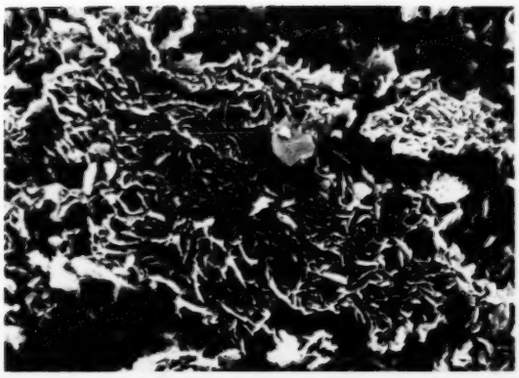

Figure 29. Scanning electron micrograph showing lamellar morphology characteristic of highly diagenetically evolved glauconite. Core B626 at 9,391 ft. Field length 26 mm.

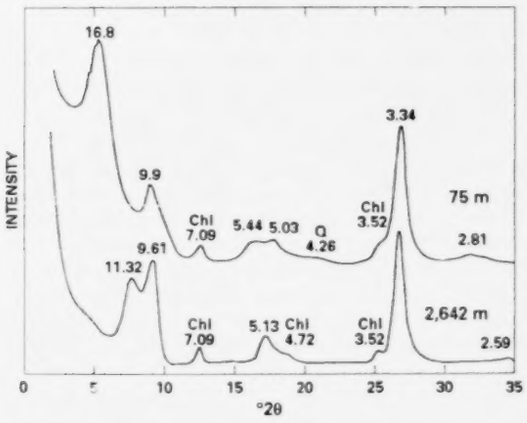

Figure 30. Typical X-ray diffraction profiles of glycol-saturated, oriented specimens of the <2-μm fraction of interstratified glauconite-smectite of representative samples from shallow and deep sandstones in the Shannon Sandstone Beds. The shallow samples (upper profile, present depth 75 m, 55 percent smectite layers) exhibit a higher proportion of smectite layers in the interstratified glauconite than do the more deeply buried samples (lower profile, present depth 2,642 m, 10 percent smectite layers). Cu Kα radiation; peak positions in angstroms. Chl, chlorite; Q, quartz; unlabeled peaks are glauconite-smectite.

Shannon was found to contain significantly more detrital dolomite than the Eagle (as much as 15 percent). Another source, therefore, is required to have provided dolomite to the Shannon, or, alternatively, reworking by currents may have concentrated dolomite in Shannon sand ridges.

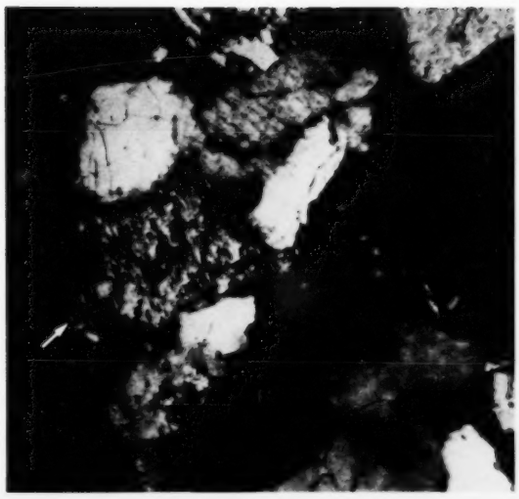

Figure 31. Photomicrograph of chessboard albite (arrow). Core A771 at 9,457 ft. Crossed nicols; field length 0.5 mm.

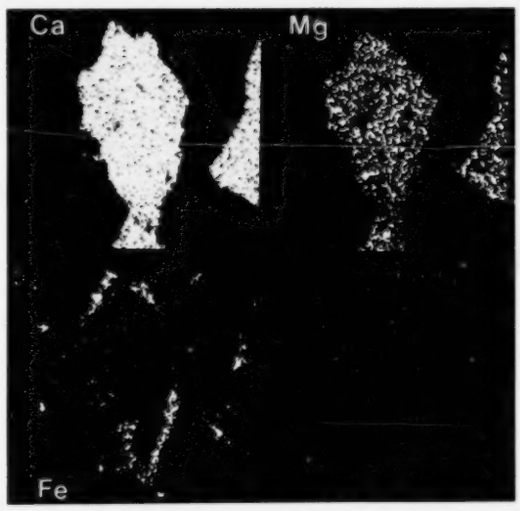

Figure 32. Scanning electron X-ray fluorescence micrographs (Ca, Mg, Fe) of ferroan dolomite overgrowth (Fe) on detrital dolomite grain. Core A771 at 9,475 ft. Field length 0.12 mm.

Petrology of Outcrop and Core Sandstones

The framework mineralogy of outcropping sandstones of the Shannon (such as at Salt Creek, Hammond, Horse Creek, and Oak Creek, fig. 1) is

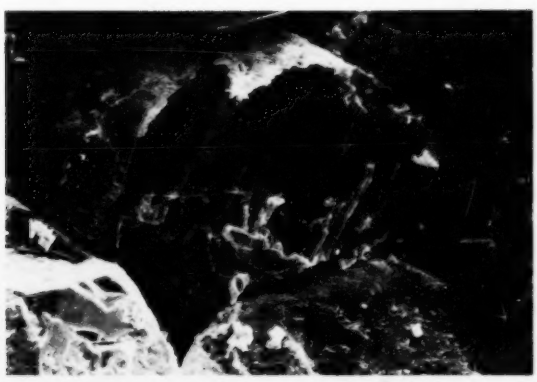

Figure 33. Scanning electron micrograph of skeletal plagioclase grain. Core C221 at 269.2 ft. Field length 0.23 mm.

similar to that of deeply buried core sandstones, but the diagenetic history is in general much simpler. Outcropping sandstones tend to be tightly cemented with early poikilotopic calcite cement that makes up as much as 30 percent by volume of the rock, and framework grains generally have point contacts. In samples from the Groat Sandstone Bed, the calcite cement is ferroan. Porosity is rare in the Groat except for minor dissolution of framework grains, especially plagioclase. Dissolution of plagioclase postdated precipitation of calcite cement because skeletal plagioclase grains are not crushed and are not filled with calcite. At Hammond, the Groat is characterized by potassium feldspar overgrowths that were precipitated before ferroan calcite cement and by a later generation of pore-filling, nonferroan calcite cement. At Salt Creek, secondary porosity is best developed in the upper part of the Shannon, hematitic grain coatings are common, and late, coarsely crystalline kaolinite locally fills vugs formed by dissolution of grains or cement.

Authigenic chlorite, less expandable glauconite-smectite, and secondary overgrowths of quartz, albite, dolomite, and siderite compose a suite of minerals characteristic of sandstones that have been deeply buried. Precipitation of these minerals is interpreted to have occurred just prior to or at about the same time as the migration of organic acids and oil into these sandstones. Sandstones of the Shannon that are now at or near the surface in the Salt Creek area were never buried deeply enough for these minerals characteristic of deeper burial to precipitate (see following section on diagenesis and paragenesis).

In a study to determine whether reservoir quality (porosity and permeability) of a particular depositional facies in the subsurface could be assessed by examining surface sandstones in the Shannon, Jackson and others (1987) found that facies in outcrop sandstones from the Salt Creek locality have sedimentological properties (and thus reservoir properties) similar to the same facies in shallowly buried sandstones from the Teapot Dome oil field; however, they did not examine deeply buried (>2,500 m) sandstones. As shown by data in our study, shallowly buried (<100 m) and outcropping sandstones have similar diagenetic histories; thus, extrapolation of reservoir properties from outcropping to shallowly buried sandstones is valid. Extrapolations from outcropping to deeply buried sandstones is invalid, however, because of the vastly different diagenetic history of deeply buried sandstones.

Diagenesis and Paragenesis

The paragenesis of authigenic minerals as inferred by their textural relations is shown on figure 35. Early diagenesis was highlighted by the precipitation of carbonate minerals—calcite in most sands and siderite where conditions were extremely reducing and alkaline and $[SO_4^{2-}]$ was low and $[Fe^{2+}]$ was high. The two samples containing apparently early calcite cement have very negative $\delta^{18}O$ values typical of calcite precipitated from meteoric water. Perhaps the calcite that precipitated early and filled primary pores recrystallized during later diagenesis in waters that were fresh, rather than brackish or saline. The only other reasonable process by which light oxygen isotopes could have been produced is by meteoric waters during early diagenesis. It is difficult, however, to envision meteoric waters migrating into (far) offshore sands of the Shannon unless sea level dropped after Shannon deposition, and there is no evidence for such a drop. Some calcite precipitated later because it fills pores that are rimmed by chlorite and by quartz and albite overgrowths. Radial extinction of ferroan calcite cement in the Groat Sandstone Bed suggests that the calcite replaced early aragonite or magnesium calcite cement.

In marine sediments, siderite commonly forms below the zone of sulfate reduction during methanogenesis after sulfate has been depleted in the formation of pyrite (Curtis and others, 1986). The $\delta^{13}C$ values of carbon in bedded siderite in this study are in the lower part of the range (-4 to +11 per mil) of methanogenic siderite. The siderite may contain a mixture of CO_2 derived from sulfate reduction or from some other process (that is, oxidation of methane). Alternatively, the siderite could have been deposited in a fresh- or brackish-water environment and redistributed into the Shannon. A probable source of iron for authigenic siderite cement was the early alteration of abundant detrital biotite and chlorite in the Shannon. Most pyrite probably formed during sulfate reduction early in diagenesis

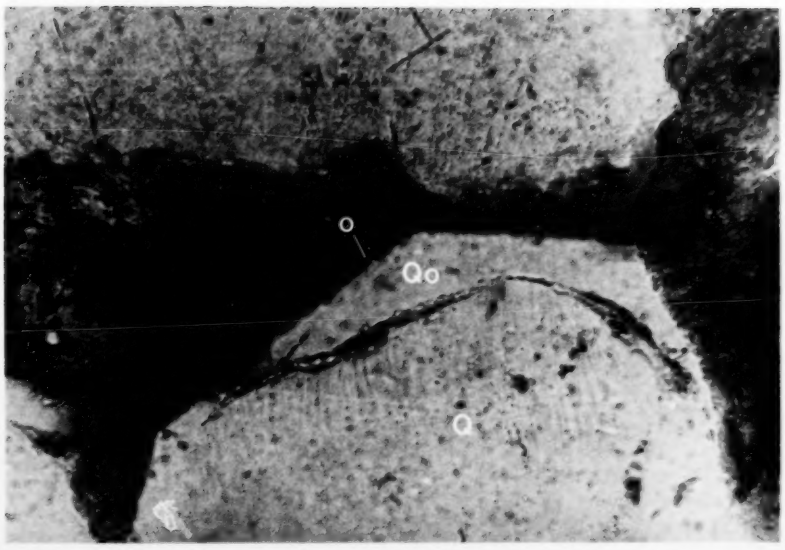

Figure 34. Photomicrograph of oil (o) between detrital quartz grain (Q) and quartz overgrowth (Qo) in secondary pore (blue); brown material under quartz overgrowth is authigenic chlorite. Core D568 at 9,512 ft. Plane-polarized light; field length 0.2 mm.

Table 5. Stable isotope values ($\delta^{18}O$ and $\delta^{13}C$) for calcite, dolomite, and siderite in Shannon Sandstone Beds

[Sample number is core designation and depth. Samples shown by location in fig. 1 and described in table 1. $\delta^{13}C$ in PDB, $\delta^{18}O$ in SMOW. Leaders (--) indicate not determined]

Sample number	Lithology	$\delta^{13}C$ (per mil)	$\delta^{18}O$ (per mil)
A771-9,457	Siderite pebble	-14 45	---
D-9,507	Siderite pebble	-12.39	---
D-9,513.5	Siderite pebble	-12.95	---
C651-10,195[1]	Bedded siderite	-7.05	-2.25
A915-9,352.7[1]	Siderite pebble	-9.04	-2.61
A729-8,617.8[1]	Siderite pebble	-9.59	-2.49
A915-9,355[1]	Bedded siderite	-5.92	-0.85
C652-10,828	Detrital dolomite	-2.65	-6.10
C221-300	Detrital dolomite	-4.20	-4.64
SC-4	Calcite cement	-12.72	-12.25
C221-253.8	Calcite cement	-10.61	-12.00

[1]Isotope values measured by A.K. Vuletich, U.S. Geological Survey; all other values measured by Global Geochemistry Corporation.

(Berner, 1971), but some (as evidenced by pyrite overlying chlorite) apparently precipitated later in reducing conditions that accompanied oil migration in shallowly buried sandstones.

Textural relations suggest that chlorite precipitation began before and continued during quartz overgrowth formation. Chlorite precipitated at about the same time as dolomite and albite overgrowths formed. Because chlorite is not found in outcropping or near-surface sandstones, which have not been deeply buried, it evidently formed during burial diagenesis. Fluids related to petroleum generation and migration may have provided some ions required for the formation of chlorite.

Precipitation of albite is inferred to have preceded calcite cementation because most plagioclase grains are albitized rather than replaced by calcite. If the plagioclase had not been albitized, it would have preferentially been replaced by calcite before potassium feldspar because plagioclase is more soluble than potassium feldspar under normal burial diagenetic conditions (Garrels and Christ, 1965). Growth boundaries between quartz and albite overgrowths indicate that these minerals were cogenetic. Potassium feldspar overgrowths in the Groat Sandstone Bed underlie ferroan carbonate cement and thus precipitated somewhat earlier than the carbonate cement.

The initial mineral composition of the glauconite was smectitic interstratified glauconite-smectite. The generally inhomogeneous and poorly crystalline mineral composition explains the commonly diffuse nature of glauconite X-ray powder diffraction patterns. As temperature and pressure increased during burial diagenesis, glauconite-smectite became more micaceous, in much the same way as the illite-smectite series (Ireland and others, 1983). Thus, the decreased expandability of glauconite-smectite in deeper samples of the Shannon is

Figure 35. Paragenesis of diagenetic alterations in the Shannon Sandstone Beds in the west-central part of the Powder River Basin.

probably a result of burial diagenesis. The exact mechanism of this reaction is not well understood, however, and the extent of reaction cannot be used as a precise thermal indicator. In an iron-rich environment, soluble organic species related to petroleum generation and migration may play an important role in the glauconite-smectite reaction.

Textural relations indicate that secondary porosity developed after precipitation of calcite, chlorite, and various types of overgrowths but before migration of oil into sandstone reservoirs. Ions (for example, Mg^{2+} and Ca^{2+}) released during the conversion of expandable glauconite-smectite to less expandable glauconite-smectite may have facilitated formation of dolomite. Iron incorporated into ferroan cements may have been derived from degradation of iron-rich biotite and chlorite. Grains and overgrowths may have been etched by organic acid- and carbonic acid-bearing pore fluids just prior to the migration of oil (MacGowan and Surdam, 1988). Concentrations of organic acid anions as high as

10,000 ppm have been measured in oil-field brines (Carothers and Kharaka, 1978). Dissolution of aluminosilicate framework grains and carbonate cements by organic acids in the subsurface has been shown to occur at burial diagenetic temperatures (80–100 °C; Surdam and others, 1984). Dissolution of quartz grains by organic acid-bearing fluids of neutral pH has also been shown to occur at ambient temperatures (Bennett and Siegel, 1987).

The presence of oil in large secondary pores indicates that oil migrated into Shannon reservoirs relatively late in the diagenetic history. Some investigators have suggested that the Cody Shale contained the source beds for oil in Shannon reservoirs, whereas others have contended that Lower Cretaceous shales were sources for most Upper Cretaceous oil (Momper and Williams, 1984). Unfortunately, burial history reconstructions do not constrain the timing of oil generation for the Cody: kinetic and time-temperature modeling indicates that oil generation occurred between 47 and 30 Ma, whereas vitrinite reflectance data suggest that the Cody was not capable of generating oil until maximum burial, about 10 Ma, and is still within the oil window (Nuccio, 1990). In the Steele Member just below shallow sandstone reservoirs in the Shannon at Teapot Dome, relatively low vitrinite reflectance values (about 0.4; Nuccio, 1990) indicate that maximum temperatures were less than 100 °C.

The paragenesis of minor phases is difficult to determine. In sample A232–9,540, however, barite cement apparently postdates calcite cement. In shallow samples late euhedral pyrite and kaolinite are present together in large secondary pores. Both pyrite and kaolinite form in acidic conditions (Garrels and Christ, 1965), and pore water may have been rendered acidic by the presence of organic acids and dissolved CO_2 associated with the migration of oil. The incursion of meteoric water into these shallow samples probably oxidized many pyrite euhedra to iron-oxide pseudomorphs of pyrite.

Depositional Environment

Mid-Shelf Model

Aspects of Shannon sand ridges (and other mid-shelf sand ridges) that are not satisfactorily explained by the mid-shelf model include siderite clasts and glauconite in the same facies, large siderite clasts, coal fragments and partings, abrupt facies changes, general upward coarsening of grain size, abundant detrital dolomite, and siderite shale barren of foraminifera within the Shannon. Other aspects of mid-shelf sand ridges, such as the dynamics of ridge formation on the shelf, have been questioned by many authors (see Stubblefield and others, 1984).

The apparently anomalous occurrence of glauconite (oxidizing/reducing conditions) and siderite (extremely reducing) in the coarsest crossbedded sandstones has been explained by multiple periods of erosion and redeposition of sand-ridge facies by shelf currents (Gaynor and Swift, 1988). Siderite and shale rip-up clasts formed when storm currents eroded bedded siderite (formed during early diagenesis) and shale in previously formed sand-ridge facies. These clasts were then redeposited in newly formed sand-ridge facies (Tillman and Martinsen, 1984; Gaynor and Swift, 1988). Some siderite and coal fragments may have been rafted onto the shelf by longshore and storm currents. Gaynor and Swift (1988) described sand ridges as being formed by a series of erosional and depositional events. They interpreted the common abrupt facies changes between sideritic and glauconitic medium-grained sandstone and shale as marking erosion surfaces that were created on the up-current sides of sand ridges by the strong action of shelf currents.

Some proponents of the mid-shelf model have proposed that upward-coarsening grain size in the Shannon is related to episodic tectonic activity along the Sevier orogenic belt far to the west (Swift, 1985). During each pulse of thrust faulting, increased sediment supply and decreased water depths in the Campanian seaway resulted in upward-coarsening sequences. Gaynor and Swift (1988) described coarsening in upper shoreward facies as a product of current action.

The abundance of slightly abraded dolomite in Shannon sand ridges, which are inferred to have been deposited more than 100 km from land, requires a particular set of circumstances because dolomite clasts can tolerate only a slight reworking before being significantly abraded. In the mid-shelf model, storm currents would have to transport dolomite rapidly onto the shelf with a minimum of abrasion to avoid destruction of grains.

Sideritic shale barren of foraminifera within the Shannon is difficult to account for in the context of the present mid-shelf model. Perhaps abnormal salinities and (or) depleted oxygen levels resulting from the restriction of the Cretaceous seaway limited the diversity of fauna.

For the mid-shelf model to be viable, the points discussed in this section must be satisfactorily explained. Although many dynamic sedimentological aspects of the formation of sand ridges have been elucidated carefully by the model presented by Gaynor and Swift (1988), an alternative model for sand-ridge formation should also be considered.

Alternative Model

Interpretations of the depositional environment of linear marine Cretaceous sandstones and modern mid-shelf sand bodies have been modified in light of new concepts in event stratigraphy and eustatic fluctuations (Plint and others, 1986, 1987; Downing and Walker, 1988). Some geologists advocate that mid-shelf sand ridges were once part of a shoreline sequence (for example, shoreface or barrier island) that was degraded during a transgression and then reworked during a post-transgressive period on the shelf (Kiteley and Field, 1984; Stubblefield and others, 1984). In this model, modern linear sand ridges on the Atlantic shelf are interpreted to be submerged barrier islands or shoreface remnants rather than actively forming shelf ridges (Rampino and Sanders, 1980; Stubblefield and others, 1984). Likewise, linear sand ridges of the upper Albian Viking Formation in Alberta, formerly thought to be mid-shelf bars, have been reinterpreted as relict shoreface sand bodies that were reworked by tidal currents and wave action during a sea-level transgression and redeposited as ridges in 5–15 m of water (Downing and Walker, 1988). In northeastern Colorado, the Hygiene Sandstone Member, which is enclosed in the marine Pierre Shale, was originally deposited in a nearshore setting and then reworked by southerly storm currents (Kiteley and Field, 1984).

Most of these sand ridges, including the Viking Formation and Turonian Cardium Formation of Alberta, are marked by numerous erosional unconformities (Bergman and Walker, 1986; Plint and others, 1986; Downing and Walker, 1988). These sand bodies are commonly overlain and underlain by erosion (transgression) surfaces (Plint and others, 1986) that are made obvious in some areas by rapid facies changes, deep scouring (for example, 20 m of relief), and pebble beds several meters thick. Subsurface correlations by Plint and others (1986) show additional subtle erosion surfaces in the Cardium that are only recognizable by "sideritic horizons with a scattering of granules or coarse to very coarse sand grains."

Weimer (1983) stated that two major criteria for the recognition of unconformities caused by eustatic changes are (1) missing facies in a normal regressive sequence and (2) phosphatic nodules and glauconite on scour surfaces. Phosphatic pebbles are near the base of the Shannon at several localities (Spearing, 1976) and were noted in one of the cores of the present study. This phosphatic zone at the base of the Shannon has been interpreted to be a regional transgressive disconformity (Gaynor and Swift, 1988).

The most favorable environment of formation for siderite is fresh to brackish water that has high alkalinity, low sulfate activity, and low oxygen content (Garrels and Christ, 1965) in swampy, coal-bearing lagoonal or deltaic-estuarine settings (Curtis and others, 1986). Siderite is not common in normal marine sedimentary rocks (Ellwood and others, 1988) and where present may be a product of methanogenesis; however, stable isotope values on carbon in siderite clasts of this study are not characteristic of methanogenic carbonate. If Shannon sand bodies were originally deposited on the shelf as shoreline facies during a regression, then the siderite could indeed be a product of lagoonal, estuarine, or deltaic deposition, affording an explanation for the large size and abundance of the clasts and light $\delta^{13}C$ values. Likewise, coal fragments could have been derived from reworking of a nonmarine facies and coal partings, and sideritic shales within the Shannon could be remnants of backbeach or deltaic facies. Stubblefield and others (1984) proposed that interlayered mud and fine sand in modern mid-shelf sand ridges was deposited in backbeach or shoreface facies.

Many characteristics of Shannon sand ridges can be explained by this alternative depositional model. The absence of typical shoreface trace fossils such as *Ophiomorphia* is not proof that the Shannon was not originally part of a shoreline sequence because trace fossils could have been obliterated in the reworking process. In addition, the abundance of glauconite may not indicate original deposition on the mid- to outer shelf because glauconite could have been picked up by the transgressing sea and incorporated into reworked shoreline sand bodies. Some dolomite may have been derived from nearby tidal flats alleviating the problem of long-distance transport. The impoverished fauna in shales of the Shannon may be, in part, an artifact of intense reworking by currents. The near absence of plant fragments, which are common in a lagoonal or estuarine setting, may be due to current winnowing.

CONCLUSIONS

The Shannon Sandstone Beds in the Powder River Basin are chert- and glauconite-rich litharenites. The abundance of sedimentary rock fragments (chert, dolomite, and fine-grained clastic fragments) and the paucity of labile heavy-mineral species suggest that source rocks were primarily sedimentary and (or) that source areas were a long distance to the west. Major diagenetic differences exist between sandstones now on the surface or shallowly buried and deeply buried sandstones. Authigenic chlorite, quartz, and albite did not form in shallow reservoir sandstones because, as vitrinite reflectance values indicate, the sandstones have never been deeply buried.

Pervasive secondary porosity, dissolved potassium feldspars, and etched quartz grains in reservoir sandstones may have developed in response to the migration of organic acid-bearing fluids through deeply

buried sandstones just prior to the emplacement of oil. Dissolution of aluminosilicate minerals provided ions for the formation of secondary minerals such as quartz and albite that grew into secondary pores. Oil migrated from Cretaceous source beds (possibly the Cody Shale) into Shannon reservoirs late in the postdepositional history of the Shannon as indicated by textural relations between oil and other diagenetic phases and by burial history modeling.

A synthesis of petrologic, sedimentologic, and paleontologic data from this and other studies suggests that rather than having been originally deposited on the middle shelf, sand ridges may be a product of a sequence of sedimentological processes: deposition of regressive (linear) shoreline facies on the shelf; degradation and reworking of sand bodies during a transgression; and, finally, aggradation and reworking by shelf currents and marine organisms in deeper water on the middle shelf.

REFERENCES CITED

Amsbury, D.L., 1962, Detrital dolomite in central Texas: Journal of Sedimentary Petrology, v. 32, no. 1, p. 5–14.

Bailey, S.W., 1980, Summary of recommendations of AIPEA nomenclature committee on clay minerals: American Mineralogist, v. 65, p. 1–7.

Bailey, S.W., Brindley, G.W., Fanning, D.S., Kodama, H., and Martin, R.T., 1984, Report of the Clay Minerals Society Nomenclature Committee for 1982 and 1983: Clays and Clay Minerals, v. 32, p. 239–240.

Beaumont, E.A., 1984, Retrogradational shelf sedimentation Lower Cretaceous Viking Formation, central Alberta, *in* Tillman, R.W., and Siemers, C.T., eds., Siliciclastic shelf sediments: Society of Economic Paleontologists and Mineralogists Special Publication 34, p. 163–178.

Bennett, P., and Siegel, D.E., 1987, Increased solubility of quartz in water due to complexing by organic compounds: Nature, v. 326, p. 684–686.

Bergman, K.M., and Walker, R.G., 1986, Cardium Formation conglomerates at Carrot Creek field—Offshore linear ridges or shoreface deposits, *in* Moslow, T.F., and Rhodes, E.G., eds., Modern and ancient shelf clastics: Society of Economic Paleontologists and Mineralogists Core Workshop 9, p. 217–268.

Berner, R.A., 1971, Principles of chemical sedimentology: New York, McGraw-Hill, 240 p.

Carothers, W.W., and Kharaka, Y.K., 1978, Aliphatic acid anions in oil-field waters—Implications for origin of natural gas: American Association of Petroleum Geologists Bulletin, v. 62, p. 2441–2453.

——— 1980, Stable carbon isotopes of HCO_3 in oil-field waters —Implications for the origin of CO_2: Geochimica et Cosmochimica Acta, v. 44, p. 232–332.

Chamberlain, C.K., 1978, Recognition of trace fossils *in* Basan, P.B, ed., Trace fossil concepts: Society of Economic Paleontologists and Mineralogists Short Course 5, p. 119–166.

Curtis, C.D., Coleman, M.L., and Love, L.G., 1986, Pore water evolution during sediment burial from isotopic and mineral chemistry of calcite, dolomite, and siderite concretions: Geochimica et Cosmochimica Acta, v. 50, p. 2321–2334.

Downing, K.P., and Walker, R.G., 1988, Viking Formation, Joffre Field, Alberta—Shoreface origin of long, narrow sand body encased in marine mudstones: American Association of Petroleum Geologists Bulletin, v. 72, no. 10, p. 1212–1228.

Ellwood, B.B., Chrzanowski, T.H., Hrouda, F., Long, G.J., and Buhl, M.L., 1988, Siderite formation in anoxic deep-sea sediments—A synergetic bacterially controlled process with important implications in paleomagnetism: Geology, v. 16, p. 980–982.

Folk, R.L., 1974, Petrology of sedimentary rocks: Austin, Texas, Hemphill's, 182 p.

Garrels, R.M., and Christ, C.L., 1965, Solutions, minerals, and equilibria: New York, Harper and Row, 450 p.

Gautier, D.L, 1981a, Petrology of the Eagle Sandstone, Bearpaw Mountains area, north-central Montana: U. S. Geological Survey Bulletin 1521, 54 p.

——— 1981b, Lithology, reservoir properties, and burial history of portion of Gammon Shale (Cretaceous), southwestern North Dakota: American Association of Petroleum Geologists Bulletin, v. 65, no. 6, p. 1146–1159.

Gaynor, G.C., and Swift, D.J.P., 1988, Shannon sandstone depositional model—Sand ridge dynamics on the Campanian Western Interior shelf: Journal of Sedimentary Petrology, v. 58, no. 5, p. 868–880.

Gill, J.R., and Burkholder, R.E., 1979, Measured sections of the Montana Group and equivalent rocks from Montana and Wyoming: U.S. Geological Survey Open-File Report 79–1143, 202 p.

Gill, J.R., and Cobban, W.A., 1973, Stratigraphy and geologic history of the Montana Group and equivalent rocks, Montana, Wyoming and North Dakota: U.S. Geological Survey Professional Paper 776, 37 p.

Haq, B.U., Hardenbol, Jan, and Vail, P.R., 1987, Chronology of fluctuating sea levels since the Triassic: Science, v. 235, p. 1156–1167.

Hardie, L.A., 1987, Dolomitization—A critical view of some current views: Journal of Sedimentary Petrology, v. 57, no. 1, p. 166–183.

Hose, R.K., 1955, Geology of the Crazy Woman Creek area, Johnson County, Wyoming: U.S. Geological Survey Bulletin 1027-B, p. 33–118.

Huthnance, J.M., 1982, On one mechanism forming linear sand banks: Estuarine, Coastal, and Shelf Science, v. 14, p. 79–99.

Ireland, B.J., Curtis, C.D., and Whiteman, J.A., 1983, Compositional variation within some glauconites and illites and implications for their stability and origins: Sedimentology, v. 30, p. 769–786.

Jackson, S.R, Szpakiewicz, M., and Tomutsa, L., 1987, Geological characterization and statistical comparison of outcrop and subsurface facies—Shannon shelf sand ridges: National Institute for Petroleum and Energy Research Report NIPER–214, 62 p.

Keefer, W.R., 1974, Geologic map of the northern Great Plains: U.S. Geological Survey Open-File Report 74–50, 3 p.

Kiteley, Louise, and Field, Mike, 1984, Shallow marine depositional environments in the Upper Cretaceous of northern Colorado, *in* Tillman, R.W., and Siemers, C.T., eds., Siliciclastic shelf sediments: Society of Economic Paleontologists and Mineralogists Special Publication 34, p. 179–204.

Land, L.S., 1980, The isotopic and trace element geochemistry of dolomite—The state of the art, *in* Zenger, D.H., Dunham, J.B., and Ethington, R.L., eds., Concepts and models of dolomitization: Society of Economic Paleontologists and Mineralogists Special Publication 28, p. 87–110.

Longstaffe, F.J., 1988, Stable isotope studies of diagenetic processes, *in* Kyser, T.K., ed., Stable isotope geochemistry of low temperature processes: Mineralogical Association of Canada Short Course Handbook, v. 13, p. 187–257.

MacGowan, D.B., and Surdam, R.C., 1988, Difunctional organic acid anions in oilfield waters: Organic Geochemistry, v. 12, no. 3, p. 245–259.

Mapel, W.J., 1959, Geology and coal resources of the Buffalo–Lake DeSmet area, Johnson and Sheridan Counties, Wyoming: U.S. Geological Survey Bulletin 1078, 148 p.

McCrea, J.M., 1950, On the isotope chemistry of carbonates and a paleotemperature scale: Journal of Chemistry and Physics, v. 18, p. 849–857.

McRae, S.G., 1972, Glauconite: Earth-Science Review, v. 8, p. 397–440.

Momper, J.A., and Williams, J.A., 1984, Geochemical exploration in the Powder River Basin, *in* Demaison, G., and Murris, R.J., eds., Petroleum geochemistry and basin evolution: American Association of Petroleum Geologists Memoir 35, p. 181–192.

Nuccio, V.F., 1990, Burial, thermal, and petroleum generation history of the Upper Cretaceous Steele Shale Member of the Cody Shale (Shannon Sandstone Bed horizon), Powder River Basin, Wyoming: U.S. Geological Survey Bulletin 1917–A.

Odin, G.S., and Fullagar, P.D., 1988, Geological significance of the glaucony facies, *in* Odin, G.S., ed., Green marine clays: Amsterdam, Elsevier, p. 295–332.

Odin, G.S., and Morton, A.C., 1988, Authigenic green particles from marine environments, *in* Chilingarian, G.V., and Wolf, K.H., eds., Diagenesis, II—Developments in Sedimentology 43: Amsterdam, Elsevier, p. 213–264.

Plint, A.G., Walker, R.G., and Bergman, K.M., 1986, Cardium Formation 6—Stratigraphic framework of the Cardium in subsurface: Bulletin of Canadian Petroleum Geology, v. 34, no. 2, p. 213–225.

_____ 1987, Cardium Formation 6—Stratigraphic framework of the Cardium in subsurface; reply: Bulletin of Canadian Petroleum Geology, v. 35, p. 365–374.

Rampino, M.R., and Sanders, J.E., 1980, Holocene transgression in south-central Long Island, New York: Journal of Sedimentary Petrology, v. 50, p. 1063–1079.

Ranganathan, Vishnu, and Tye, R.S., 1986, Petrography, diagenesis, and facies controls on porosity in Shannon Sandstone, Hartzog Draw Field, Wyoming: American Association of Petroleum Geologists Bulletin, v. 70, no. 1, p. 56–69.

Rice, D.D., and Shurr, G.W., 1983, Patterns of sedimentation and paleogeography across the Western Interior seaway during time of deposition of Upper Cretaceous Eagle Sandstone and equivalent rocks, northern Great Plains, *in* Reynolds, M.W., and Dolly, E.D., eds., Mesozoic paleogeography of the west-central United States: Society of Economic Paleontologists and Mineralogists Rocky Mountain Paleogeography Symposium 2, p. 337–358.

Sabins, F.F., Jr., 1962, Grains of detrital, secondary, and primary dolomite from Cretaceous strata of the Western Interior: Geological Society of America Bulletin, v. 73, p. 1183–1196.

Seeling, Alan, 1978, The Shannon Sandstone, a further look at the environment of deposition at Heldt Draw field, Wyoming: The Mountain Geologist, v. 15, no. 4, p. 133–144.

Seilacher, Adolf, 1978, Use of trace fossil assemblages for recognizing depositional environments, *in* Basan, P.B., ed., Trace fossil concepts: Society of Economic Paleontologists and Mineralogists Short Course 5, p. 167–181.

Shurr, G.W., 1984, Geometry of shelf sandstone bodies in the Shannon Sandstone of southeastern Montana, *in* Tillman, R.W., and Siemers, C.T., eds., Siliciclastic shelf sediments: Society of Economic Paleontologists and Mineralogists Special Publication 34, p. 63–83.

Spearing, D.R., 1976, Upper Cretaceous Shannon Sandstone—An offshore shallow-marine sand body: Wyoming Geological Association, 28th Annual Field Conference, Guidebook, p. 65–72.

Stubblefield, W.L., McGrail, D.W., Dersey, D.G., 1984, Recognition of transgressive and post-transgressive sand ridges on the New Jersey continental shelf, *in* Tillman, R.W., and Siemers, C.T., eds., Siliciclastic shelf sediments: Society of Economic Paleontologists Special Publication 34, p. 1–23.

Surdam R.C., Boese, S.W., and Crossey, L.J., 1984, The chemistry of secondary porosity, *in* McDonald, D.A., and Surdam, R.C., eds., Clastic diagenesis: American Association of Petroleum Geologists Memoir 37, p. 127–150.

Swift, D.J.P., 1985, Response of the shelf floor to flow, *in* Tillman, R.W., Swift, D.J.P., and Walker, R.G., eds., Shelf sands and sandstone reservoirs: Society of Economic Paleontologists and Mineralogists Short Course 13, p. 135–241.

Swift, D.J.P., and Rice, D.D., 1984, Sand bodies on muddy shelves—A model for sedimentation in the Western Interior Seaway, North America, *in* Tillman, R.W., and Siemers, C.T., eds., Siliciclastic shelf sediments: Society of Economic Paleontologists Special Publication 34, p. 43–62.

Swift, D.J.P., Thorne, J.A., and Oertel, G., 1986, Fluid process and sea floor response on a modern storm-dominated shelf—Middle Atlantic shelf of North America, Part II, Response of the shelf floor, *in* Knight, R.J., and McLean, J.R., eds., Shelf sands and sandstones: Canadian Society of Petroleum Geologists Memoir 11, p. 191–211.

Tillman, R.W., and Martinsen, R.S., 1984, The Shannon shelf-ridge sandstone complex, Salt Creek anticline area, Powder River basin, Wyoming, *in* Tillman, R.W., and Siemers, C.T., eds., Siliciclastic shelf sediments: Society of Economic Paleontologists and Mineralogists Special Publication 34, p. 85–142.

_____ 1985, Shannon Sandstone—Hartzog Draw Field core study, *in* Tillman, R.W., Swift, D.J.P., and Walker, R.G., eds., Shelf sands and sandstone reservoirs: Society of Economic Paleontologists and Mineralogists Short Course 13, p. 577–644.

_____ 1987, Sedimentologic model and production characteristics of Hartzog Draw Field, Wyoming, a Shannon shelf-ridge sandstone, *in* Tillman, R.W., and Weber, K.J., eds., Reservoir sedimentology: Society of Economic Paleontologists and Mineralogists Special Publication 40, p. 15–112.

Walker, T.R., 1984, 1984 SEPM Presidential address; diagenetic albitization of potassium feldspar in arkosic sandstones: Journal of Sedimentology, v. 54, no. 1, p. 3–16.

Weimer, R.J., 1983, Relation of unconformities, tectonics, and sea level changes, Cretaceous of the Denver Basin and adjacent areas, *in* Reynolds, M.W., and Dolly, E.D., eds., Mesozoic paleogeography of the west-central United States: Society of Economic Paleontologists and Mineralogists Rocky Mountain Paleogeography Symposium 2, p. 359–376.

Young, H.R., and Doig, D.J., 1986, Petrography and provenance of the Glauconitic Sandstone, south-central Alberta, with comments on the occurrence of detrital dolomite: Bulletin of Canadian Petroleum Geology, v. 34, no. 4, p. 408–425.

Appendix. Core descriptions of the Shannon Sandstone Beds of the Steele Member of the Cody Shale, Powder River Basin, Wyoming

[Drillhole locations shown in fig. 1. Interval given in feet. Facies described in table 2 and in text]

Interval	Facies	Description
		CORE D568
9,485-9,505.8	4a	Laminated, rippled shale and very fine grained sandstone; sparse burrows; maximum bed thickness, 1.5 in.
9,505.8-9,506.8	2	Rippled sandstone/shale; <15 percent shale; moderate burrowing.
9,506.8-9,508.8	1a	Moderate-angle trough crossbedded sandstone; glauconitic; shale ripups; 4–6-in.-thick zone of siderite pebbles (4-8 in. diameter) at 9,508.8 ft.
9,508.8-9,512.8	1a	Oil-stained interval; few shale ripups; one siderite clast (1.5 in.).
9,512.8-9,519.2	1a	Glauconitic, rippled, crossbedded sandstone; round siderite clasts (1 in.) at top; shale ripups.
9,519.2-9,543.5	3	Bioturbated sandstone; compacted circular burrows; locally mottled; discontinuous shale laminae (<20 percent); lenses of glauconitic fine-grained sandstone.
9,543.5-9,544	4b	Dark-gray shale; some very fine grained sandstone.
		CORE A232
9,526-9,554	3	Bioturbated, very fine grained, glauconitic sandstone/siltstone; clusters of Terebellina burrows; glauconitic planar laminae at 9,532 ft; rippled intervals; thin, wispy black laminae; horizontal to inclined burrows.
		CORE A729
8,580-8,582	2	Burrowed sandstone; Terebellina burrows; shale ripups.
8,582-8,582.5	1a	Moderate-angle crossbedded, glauconitic sandstone; shale ripups.
8,582.5-8,587.3	2	Burrowed, rippled sandstone/shale; long vertical burrows (2 in.); horizontal burrows; 3-in.-thick sandstone intervals.
8,587.3-8,590	1a	Crossbedded sandstone; low-angle troughs; shale ripups; one siderite pebble (1 in.).
8,590-8,592.6	2	Burrowed sandstone/shale.
8,592.6-8,594	1a	Rippled sandstone; sparse shale ripups.
8,594-8,607	2	Burrowed sandstone/shale; rippled.
8,607-8,618	1a	Low to moderate-angle crossbedded, glauconitic sandstone; rippled; abundant shale ripups; sparse horizontal burrows; siderite zone at 8,617.8 ft.
		CORE C221
245-253.2	4b	Massive silty shale/sandstone.
253.2-254.8	1a	Moderate- to high-angle crossbedded sandstone; very glauconitic.
254.8-366	1a	Oil-stained, rippled sandstone; abundant ripups; local bioturbated sandstone and wavy shale laminae; siderite at 346.5 ft; local burrows; 3-in.-thick mottled layer at 263.5 ft; shalier toward base.
		CORE B626
9,365-9,379	3	Bioturbated sandstone/shale; shalier towards base.
9,379-9,389.3	4a	Laminated silty shale; sparse to moderate burrows.
9,389.3-9,395.2	1a	Low-angle crossbedded, rippled sandstone; siderite pebbles at top flattened along bedding; coarse glauconite pellets; shale ripups; sparse pebbles; thin burrowed intervals.
9,395.2-9,419	3	Burrowed, rippled sandstone/shale; long, vertical burrows; some intervals are bioturbated.
		CORE A771
9,415-9,439	4a	Laminated silty shale; sparse burrows.
9,439-9,462	1a	Medium-grained, glauconitic, oil-stained sandstone; siderite pebbles and clay ripups; zones of siderite pebbles (as large as 4 in.) at top and base.
9,462-9,480	3	Bioturbated sandstone/shale; sharp facies break between this unit and unit above; abundant horizontal and vertical burrows.
		CORE C651
10,193-10,198	4a	Laminated, rippled, dark-gray shale; sparse burrows; 1.5-in.-thick bedded siderite at 10,195 ft.
10,198-10,208	2	Burrowed sandstone/shale; thin intervals of crossbedded sandstone; vertical burrows.
10,208-10,216	1a	Low-angle crossbedded sandstone; some planar laminae; sparse siderite pebbles.
10,216-10,225	2	Burrowed sandstone/shale; rippled.
10,225-10,242	1a	Low- to high-angle crossbedded sandstone; abundant shale ripups locally; siderite at 10,227 and 10,235 ft; a few intervals of burrowed sandstone.
10,242-10,253	2	Bioturbated/burrowed sandstone/shale; long vertical burrows; some horizontal burrows.
		CORE C652
10,796-10,829	2	Burrowed, rippled sandstone/shale; U-shaped burrow at 10,796 ft; sand lenses (1-3 in. thick); long (>1 in.) vertical burrows common.
10,829-10,840	4a	Black, laminated shale; rare burrows; bedded siderite at 10,831.8 ft; dolomitic from 10,830 to 10,832 ft (X-ray identification).

Appendix. Continued

Interval	Facies	Description
		CORE A817
9,885-9,892	2	Burrowed sandstone/shale; sparse vertical burrows; rippled.
9,892-9,897.8	3	Bioturbated sandstone; abundant vertical burrows.
9,897.8-9,918.4	1b	Very fine grained sandstone; few ripups, pebbles, or crossbeds; 2 1-in.-diameter siderite pebbles at 9,913.5 ft; glauconitic, planar laminae at 9,918 ft.
9,918.4-9,947	2	Burrowed sandstone/shale; shalier at base; rippled; sparse burrows in some intervals; horizontal and inclined burrows; coal partings from 9,920.6 to 9,920.8 ft.
		CORE A915
9,325-9,346.5	4a	Laminated black shale and minor sandstone; rare inclined burrows; 5-in.-thick, very fine grained sandstone at 9,339.2 ft.
9,346.5-9,348.5	1a	Fine-grained sandstone; abundant shale ripups; 1-in.-thick siderite bed at top.
9,348.5-9,351.5	2	Burrowed sandstone/shale; vertical and inclined burrows.
9,351.5-9,353.2	1a	Glauconitic sandstone; low-angle crossbeds; siderite at base; coal fragment at 9,352 ft.
9,353.2-9,354	2	Burrowed sandstone/shale; vertical and inclined burrows; brown-green clay clast (nonmarine?) at 9,353.8 ft.
9,354-9,358	4a	Laminated shale/sandstone; minor inclined burrows; 4-in.-thick siderite bed at 9,355 ft.
9,358-9,384.5	4b	Massive silty gray shale; no burrows; rippled.

☆☆ U.S. GOVERNMENT PRINTING OFFICE: 1991—573-866

DEPARTMENT OF THE INTERIOR
U.S.
March 3, 1849

SELECTED SERIES OF U.S. GEOLOGICAL SURVEY PUBLICATIONS

Periodicals

Earthquakes & Volcanoes (issued bimonthly).
Preliminary Determination of Epicenters (issued monthly).

Technical Books and Reports

Professional Papers are mainly comprehensive scientific reports of wide and lasting interest and importance to professional scientists and engineers. Included are reports on the results of resource studies and of topographic, hydrologic, and geologic investigations. They also include collections of related papers addressing different aspects of a single scientific topic.

Bulletins contain significant data and interpretations that are of lasting scientific interest but are generally more limited in scope or geographic coverage than Professional Papers. They include the results of resource studies and of geologic and topographic investigations; as well as collections of short papers related to a specific topic.

Water-Supply Papers are comprehensive reports that present significant interpretive results of hydrologic investigations of wide interest to professional geologists, hydrologists, and engineers. The series covers investigations in all phases of hydrology, including hydrogeology, availability of water, quality of water, and use of water.

Circulars present administrative information or important scientific information of wide popular interest in a format designed for distribution at no cost to the public. Information is usually of short-term interest.

Water-Resources Investigations Reports are papers of an interpretive nature made available to the public outside the formal USGS publications series. Copies are reproduced on request unlike formal USGS publications, and they are also available for public inspection at depositories indicated in USGS catalogs.

Open-File Reports include unpublished manuscript reports, maps, and other material that are made available for public consultation at depositories. They are a nonpermanent form of publication that may be cited in other publications as sources of information.

Maps

Geologic Quadrangle Maps are multicolor geologic maps on topographic bases in 7 1/2- or 15-minute quadrangle formats (scales mainly 1:24,000 or 1:62,500) showing bedrock, surficial, or engineering geology. Maps generally include brief texts; some maps include structure and columnar sections only.

Geophysical Investigations Maps are on topographic or planimetric bases at various scales; they show results of surveys using geophysical techniques, such as gravity, magnetic, seismic, or radioactivity, which reflect subsurface structures that are of economic or geologic significance. Many maps include correlations with the geology.

Miscellaneous Investigations Series Maps are on planimetric or topographic bases of regular and irregular areas at various scales; they present a wide variety of format and subject matter. The series also includes 7 1/2-minute quadrangle photogeologic maps on planimetric bases which show geology as interpreted from aerial photographs. Series also includes maps of Mars and the Moon.

Coal Investigations Maps are geologic maps on topographic or planimetric bases at various scales showing bedrock or surficial geology, stratigraphy, and structural relations in certain coal-resource areas.

Oil and Gas Investigations Charts show stratigraphic information for certain oil and gas fields and other areas having petroleum potential.

Miscellaneous Field Studies Maps are multicolor or black-and-white maps on topographic or planimetric bases on quadrangle or irregular areas at various scales. Pre-1971 maps show bedrock geology in relation to specific mining or mineral-deposit problems; post-1971 maps are primarily black-and-white maps on various subjects such as environmental studies or wilderness mineral investigations.

Hydrologic Investigations Atlases are multicolored or black-and-white maps on topographic or planimetric bases presenting a wide range of geohydrologic data of both regular and irregular areas; principal scale is 1:24,000 and regional studies are at 1:250,000 scale or smaller.

Catalogs

Permanent catalogs, as well as some others, giving comprehensive listings of U.S. Geological Survey publications are available under the conditions indicated below from the U.S. Geological Survey, Books and Open-File Reports Section, Federal Center, Box 25425, Denver, CO 80225. (See latest Price and Availability List.)

"Publications of the Geological Survey, 1879-1961" may be purchased by mail and over the counter in paperback book form and as a set of microfiche.

"Publications of the Geological Survey, 1962-1970" may be purchased by mail and over the counter in paperback book form and as a set of microfiche.

"Publications of the U.S. Geological Survey, 1971-1981" may be purchased by mail and over the counter in paperback book form (two volumes, publications listing and index) and as a set of microfiche.

Supplements for 1982, 1983, 1984, 1985, 1986, and for subsequent years since the last permanent catalog may be purchased by mail and over the counter in paperback book form.

State catalogs, "List of U.S. Geological Survey Geologic and Water-Supply Reports and Maps For (State)," may be purchased by mail and over the counter in paperback booklet form only.

"Price and Availability List of U.S. Geological Survey Publications," issued annually, is available free of charge in paperback booklet form only.

Selected copies of a monthly catalog "New Publications of the U.S. Geological Survey" available free of charge by mail or may be obtained over the counter in paperback booklet form only. Those wishing a free subscription to the monthly catalog "New Publications of the U.S. Geological Survey" should write to the U.S. Geological Survey, 582 National Center, Reston, VA 22092.

Note.--Prices of Government publications listed in older catalogs, announcements, and publications may be incorrect. Therefore, the prices charged may differ from the prices in catalogs, announcements, and publications.